ABSTRACT

Title of Document: STEREOSCOPIC VISION IN UNMANNED AERIAL VEHICLE SEARCH AND RESCUE

Ryan Collins, Joshua Gaus, Kathryn Jahn, Michael Jurrens, Saimouli Katragadda, Kaitlin Krejcik, Xincheng Li, Eileen Liu, Colin McNulty, Benedict Mondal, Matthew Weston-Dawkes, Tiffany Yen

Directed By: Dr. Anil Deane, Institute for Physical Science and Technology

Search and rescue operations are challenging due to the hazards imposed on the rescue teams. Team ARM IT has developed a virtual reality interface that controls a mounted camera payload on an unmanned aerial vehicle (UAV) through a head mounted display. This allows rescuers to manipulate a UAV to assist search and rescue missions safely and effectively through telepresence and enhanced situational awareness. The team tested these hypotheses by prototyping, testing, and refining individual components of the system through the use of flight simulation software and on-site volunteer testing. By providing a realistic sense of the UAV environment enhanced with relevant information, Team ARM IT's project reduces the danger to the rescuers and provide cognitively natural situational awareness.

STEREOSCOPIC VISION IN UNMANNED AERIAL VEHICLE SEARCH AND RESCUE

By

Ryan Collins, Joshua Gaus, Kathryn Jahn, Michael Jurrens, Saimouli Katragadda, Kaitlin Krejcik, Xincheng Li, Eileen Liu, Colin McNulty, Benedict Mondal, Matthew Weston-Dawkes, Tiffany Yen

Thesis submitted in partial fulfillment of the requirements of the Gemstone Program, University of Maryland 2018

Advisory Committee:
Dr. Anil Deane, University of Maryland, Mentor
Dr. Yiannis Aloimonos, University of Maryland
Ms. Neta Ezer, Northrop Grumman
Dr. Huan Xu, University of Maryland

Acknowledgements

Team ARM IT would like to extend thanks to several individuals and organizations that provided the support needed to complete this research. We would like to thank our mentor Dr. Anil Deane for his critical leadership and direction, and the Gemstone staff for their constant support. We would also like to thank the Laboratory for Computation and Visualization within the Institute for Physical Science and Technology (IPST) for providing lab space and funding, FedCentric for providing funding, and Northrop Grumman for providing equipment and feedback. In addition, Dr. Huan Xu, Jacob Moschler, and the University of Maryland UAS Test Site provided technical consulting and feedback that were essential to our research. We would like to acknowledge our librarian, Celina N. McDonald, for her support throughout our initial research and writing phases. Finally, we would like to thank our experts for contributing their time and feedback.

Table of Contents

List of Figures

I. Introduction

Team ARM IT sought to incorporate virtual reality (VR) and augmented reality (AR) technology into unmanned aerial vehicles (UAVs) to aid operators in Search and Rescue (SAR) operations. The theory behind utilizing this technology was to provide pilots with greater control over the camera view from the UAV and a better sense of the UAV's environment, in particular by adding natural depth perception. Relevant information can also be displayed on the video stream in the form of augmented reality overlays, which allows the operator to focus on searching for victims rather than monitoring the UAV itself.

ARM IT investigated the following research questions throughout the project: How can stereoscopic vision improve UAV operations? How does a VR and AR video feed affect operator visualization of a scene? How can a VR and AR interface improve on existing search rescue methods? By answering these questions, the team seeks to The aim of the project through the creation of a prototype system is to reduce the danger to the rescuers and provide cognitively natural situational awareness through the usage of virtual reality and stereoscopic vision.

First and foremost, ARM IT's first hypothesis posits that utilizing stereoscopic vision through an HMD will give the operator a greater sense of depth perception, resulting in better obstacle avoidance as well as a more natural view of the UAV's surrounding area. By viewing a stereoscopic camera feed through the Oculus Rift, the operator will be able to pilot the UAV with greater ease than they would be able to with a traditional UAV control setup and will have a more intuitive sense of their surroundings.

The team's second hypothesis proposes that a VR and AR video feed providing head-mounted control of a camera will allow greater control over the visualization of a particular scene. In traditional methods of UAV control, the camera is controlled by means of a joystick and provides only a monoscopic view of a particular scene. Incorporating VR and AR technology provides more information for the operator without the operator physically needing to be at the scene through the inclusion of stereoscopic vision and video feed overlays.

Finally, ARM IT hypothesizes that a VR and AR interface will greatly improve on existing search and rescue methods by allowing the operator more control over their vision and interpretation of a particular search and rescue scenario. With a VR and AR interface, the pilot will also be able to view relevant and real-time information as they control the vehicle, such as altitude, power remaining and distance from the operator. As a result of using VR and AR technology, ARM IT believes that conventional search and rescue methods will be improved and overall have a greater success rate.

II. Literature Review

A. Introduction

Team ARM IT is developing a new and advanced interface for piloting UAVs to assist in SAR operations. The objective of SAR is to locate subjects in disaster areas as quickly as possible. Disaster areas are treacherous environments, in which the sheer size and complexity of terrain pose a great challenge to SAR teams. Searching on foot can be dangerously slow in situations where time is critical, and can place the rescuers in the

same danger as the victims. Searching from manned aircraft such as planes and helicopters can allow rescuers to search a larger area in less time without endangering themselves, but the cost of these aircraft and the expertise required to pilot them can be prohibitive. UAVs allow rescuers to remain safe and require less expense to use than manned aircraft. Some rescue operations have already begun integrating UAVs into their SAR efforts. The first recorded instance of a UAV being successfully used in an SAR operation to locate and rescue victims was in January 2018 when rescuers found two boys who had been swept out to sea and dropped them a flotation device. [1] Since then, more and more SAR organizations have been utilizing UAVs in their operations due to their numerous advantages. Team ARM IT plans to build on previous successes by creating a AR/VR based interface to aid rescuers in dangerous SAR environments. The ability to manipulate a UAV allows operators to execute SAR missions safely and effectively through telepresence.

B. UAV Capabilities

SAR presents many challenges that rescue robotics can help to solve. SAR missions require the distribution of large amounts of information such as the disaster area conditions, identification of victims, and entry routes for rescuers [2]. UAVs are uniquely equipped with the capabilities to help acquire this information, as they are portable and can increase the visibility of the terrain by providing a bird's eye view [2]. This larger range of view is important in SAR missions as they eliminate the keyhole effect, in which limited views from ground SAR robots prevent their operators from understanding the environment [3].

There are also many other ways in which UAVs can help overcome the difficulties of SAR. Complex terrain does not inhibit UAV navigation since the aircraft hovers above the area. Any UAV that transmits video can aid in the location of missing persons, the assessment of a building's structural integrity, or the measurement of the extent of a forest or building fire. Additionally, the deployment of a UAV reduces any threats posed to either the rescuer or the victims, as the use of a UAV removes the operator from the scene, eliminating the risk of physical injury to the operator and the physical weight of the rescuer shifting rubble, thus avoiding further harm to the victim [4]. Other advantages that UAVs have over their human counterparts is the increased speed of response, as the UAV's high speed over complex terrain and flying capabilities allows them to navigate quickly to places that humans may have difficulty entering. This also allows the rescuers to extend the range of their response, as they can now enter previously inaccessible terrain [5].

Currently, UAV applications in disaster management include logistics and evacuation support, as UAVs can easily gather information about the victims and the rescue teams in place. Rescue missions are also a common application, where the UAVs are used to search for victims trapped by debris [6]. For such SAR missions, commercially available UAVs are a good choice due to their affordability and ease of use [6].

A survey of these commercially available UAVs shows recurring characteristics between manufacturers. Most manufacturers emphasize the "force multiplier" capability of these vehicles, which allows one or two operators to inspect larger areas of ground in a

shorter time [7-12]. On average, small UAVs are 4-6 lbs and approximately 36” across. A majority of these systems are multirotors, which are UAVs with three or more long arms with a propeller (rotor) at each end. The flight time of these systems varies from 10 minutes to an upper range of 45-60 minutes depending on battery capacity and payload [7-12]. Many systems also advertise modular payloads which can be swapped out in different situations [7-12]. The payload capacity of this UAV size ranges from 200 to 1000 grams. In its simplest form, the UAV requires only a video camera, communication modules, and flight capability. However, the surveyed UAVs often additionally include infrared imaging, and have an operational range of 1-2 km without larger upgraded antenna setups. Other useful capabilities include thermal imaging, chemical detection, and network coverage extension to assist rescuers [13]. While costs prohibit the use of these sensors in this research project, future teams may consider their usefulness.

While UAVs are a key component to improving SAR missions, there are still several problems that have yet to be solved. SAR operations generally require a human operator to control the UAVs remotely. However, human operators oftentimes have problems understanding the video feedback they are receiving. The cluttered environment from their remote feedback can often be confusing and results in a lack of situational awareness of the disaster areas [5]. Situational awareness is defined as the “perception of the elements in the environment,” the “comprehension of their meaning,” and the “projection of their status in the near future” [3]. All of these components are important in a successful SAR mission, particularly when attempting to find disaster survivors remotely. In fact, one study found that it was challenging for the operators to retain

situational awareness due to their difficulty in interpreting the remote feedback they were receiving via teleoperation [3]. According to this study, 54% of the operators were primarily occupied with the "perception and comprehension of the robot and environment" [3]. One significant factor in establishing situational awareness for operators are the user interfaces in rescue robotics. Having a complex interface will decrease the rescuer's abilities while simultaneously increasing the amount of training users need to attain proficiency. For example, during the SAR mission at the World Trade Center, one of the SAR robots available was rejected due to its over-complicated user interface [2]. The interface must be simple and intuitive enough for the user to easily determine the state of the environment that they are working in, as well as not overly clutter the operator's vision.

The two most common existing UAV control mechanisms are the tangible user interface, such as a joystick or wheel, and the graphical user interface [14]. Both these methods rely on sending and receiving information remotely to the aerial vehicle by using an onboard communication device [15]. Tangible interfaces are commonly used by both manned and unmanned aircrafts [15]. For manned aircrafts, a primary joystick controls the roll and pitch, a secondary joystick controls the thrust of the rotors, and a foot pedal controls the yaw. Larger UAVs, such as military or research vehicles, often use a setup similar to manned aircraft to accommodate pilots previously trained in manned aircraft [15]. Small UAVs, such as those used by hobbyists and videographers, use a radio control transmitter with two 2-axis joysticks. The most common control scheme maps pitch and roll control to the right stick and thrust and yaw to the left stick

[14]. Other commonly used tangible interfaces include the gamepad and the remote, which are primarily used for video games [14]. The gamepad model is a variation of the joystick model, with a combination of buttons and small joysticks mapped to vehicle functions and directional commands. The remote, on the other hand, acts as an extension of the arm, allowing a user's gestures to control the system.

Graphical user interfaces (GUI) consist primarily of computer screens designed to provide the user with information regarding the UAV, such as data streams or control systems [16]. More specifically, a GUI can be a mobile device, such as a smartphone or tablet, or a computer, such as a laptop or desktop. Mobile devices in particular are popular for controlling recreational UAVs [14]. The benefits of mobile devices as control mechanisms are their portability, universality, and compatibility with various applications. The drawbacks, however, include the small size of the screen, the lack of processing power, and the lack of feedback from the controls. The last problem is of particular importance, especially when compared to tangible control mechanisms. Due to the mobile device's touch screen features, the user loses tactile feedback received from a tangible mechanism's physical position of the control. This limitation presents a significant issue for creating more intuitive controls. On the other hand, in contrast to mobile devices, computers offer larger screens, more processing power, and more control options. However, in designing computer interfaces, these increasingly complex systems require a higher data transmission rate as more information is exchanged between the user and the UAV [16].

C. Monoscopic and Stereoscopic Vision

The objective of a search and rescue mission is essentially an object recognition problem. The human brain recognizes an object by first distinguishing the shape of the object and then profiling the object by searching for patterns that can be matched to a memory bank [17]. The first step, outlining the object, is done through visual cues such as contrast or depth perception. Depth perception is the phenomenon by which observers can distinguish the distance between layers of objects in their field of view (FOV). This increases environmental and situational awareness, which is highly desirable in SAR [18].

In humans, depth perception comes from monocular cues, such as motion, perspective, and occlusion, as well as from binocular cues, such as stereopsis [19, 20]. Stereopsis arises from the disparity between the two points of view caused by the distance between human eyes, called the interpupillary distance (IPD). By processing two images taken from different angles, the human brain can focus on an object within the eyes' FOV and, through instantaneous implicit calculations, deduce the focal length. Thus, two image projections are used to create depth perception, achieving a 3D effect from 2D imaging [21].

Images and video are generally displayed on two-dimensional monitors (AiMT), which only contribute monoscopic images and video, where the same image or video stream is provided to both eyes. However, for SAR purposes, the locations of interests and terrain are three-dimensional data. Monoscopic videos and images will lose depth information, as they can only supply monoscopic cues. In contrast, stereoscopic videos

can provide both monoscopic and stereoscopic cues. A 2004 study used a Maximum Likelihood Model to show that the reliability and accuracy of depth perception increased when both stereoscopic and monoscopic cues were made available to the observer, as the brain processes and combines the cues in a statistically optimal fashion to make up for any errors [22]. Another study has also shown stereoscopy to be a major factor in detecting an object camouflaged in an environment [23]. Indeed, incorporating stereoscopic vision more closely mimics human vision and creates a more "realistic perception" [24] when visualizing data. This is due to the fact that generating stereoscopic vision will "render the data from two slightly different perspective angles," similar to how humans perceive depth. In fact, a study that used stereoscopic vision in military exercises found that stereoscopic vision was "beneficial for reducing users' error" when compared to only using monoscopic vision, particularly in line of sight tasks. [24]. In addition, the study's survey showed that 75% of their subjects preferred using stereoscopic vision. Therefore, utilizing stereopsis in search and rescue UAVs would increase the accuracy in the depth perception of the operator.

Stereopsis is attained through the recreation of a human's binocular vision using two image sensors or cameras. A binocular system similar to that of human eyes can be constructed by positioning two cameras adjacently and orienting their lenses toward an object. The image output of each camera will be relayed to each eye through the use of an HMD. The HMD will display the images taken by the camera on the left to the user's left eye and will display the images taken by the camera on the right to the user's right eye. The interaxial distance (IAD), or the distance separating the centers of the two camera

lenses, must closely match the user's IPD in order to mimic the user's optical system [19, 20].

Two methods exist in replicating the user's optical system. The first uses readymade stereoscopic cameras (two camera modules placed on one circuit board) which eases image processing as such systems output a single stereoscopic image (two images side-by-side). These systems, however, have fixed IAD since the cameras are locked onto the baseboard and consequently do not accommodate the variance in human IPD. As human IPD varies from 52mm to 78mm, it is worthwhile for the IAD of the cameras to be adjustable to account for this variance in users of the stereoscopic system [25]. The second method, as an alternative to fixed stereoscopic cameras, places two cameras purchased separately in a stereoscopic case that holds the two cameras adjacently. This would allow freedom to adjust the IAD to match a particular user's IPD. Naturally, a high resolution camera is desirable such that the user can view the environment with enough clarity to identify small details. The optimal resolution of the camera is determined by the HMD to be used.

D. Augmented and Virtual Reality Interface

According to Fox et al., VR is a "substitute reality" where people can interact with non-real environments and objects in an exclusively digital world [26]. While virtual environments have primarily been used for gaming and immersive simulations, AR overlays computer-generated graphics onto the real world [27]. AR enhances the real world as opposed to virtual reality, which replaces the real world. AR is primarily used to enhance human performance by adding critical information to the user's view (e.g. an

aircraft pilot's heads up display) [27]. These displays not only provide additional information about a situation, but also allow the user to make real-time decisions. The Oculus Rift (Oculus) will be the main VR platform utilized in this project. The platform was initially created as a VR gaming headset but has proven to have further applications within the bounds of VR [28]. The Oculus Rift software, the System Developer's Kit (SDK), is completely free [28]. The Oculus is also compatible with the Unity and Unreal Engine gaming engines, and is most suited for the C++ programming language [29].

The major reason the Oculus was chosen for this project was for its commercial availability, relatively low cost, and open-source modification ability [29]. In addition, the Oculus provides a large range of developer's tools through its three readily available versions, two Developer's Kits (DK1 and DK2) and the Consumer Version (CV1), which are internally very similar but have significant differences [28]. The CV1 ($400) features 25% more resolution than the DK2 ($400), which in turn features about twice the visual display power of the DK1 ($250). Additionally, the DK2 and CV1 have positional tracking capabilities that the DK1 does not, which allows for more accurate registration of the user's head movements [30]. The HMD features a built-in gyroscope, accelerometer, and magnetometer which are able to read the yaw, pitch, and roll of the user's head and adjust the displayed image relative to the user's movements [28]. The later versions' additional positional tracking adds a fourth degree, allowing the user to lean in closer or further away from a point or peek around a wall. This added degree also reduces dizziness and confusion while using the headset [28]. The sampling and frame

rates of the images are extremely high in order to reduce blurriness, double imagery, and "ghosting" of the image [28]. Oculus developers highlight the necessity of using correct distorting and calibrating values while displaying the image in order to mirror human vision [31].

However, the Oculus faces many drawbacks due to the inherent nature of VR technology, which can cause disorientation and strain on the part of the user [29]. This disorientation and strain, often with symptoms very similar to motion sickness, is known as VR sickness. For example, the Oculus has a high data draw of a 1920 x 1080 resolution and 75-hz refresh rate [29] and requires two cameras of resolution 1080 pixels by 1200 pixels in order to best synchronize image data to create stereoscopic vision and avoid VR sickness [19]. This resolution will require extremely high rates of data transmission between the ground control system (GCS) and the UAV. Unnatural degrees of motion, such as sudden acceleration or strafing side to side, also have to be restricted to avoid disorientation on the part of the user, which could affect the autopilot used for the UAV [29]. Latency in the displayed images can also contribute greatly to VR sickness; Oculus developers suggest maintaining the smallest amount of variance in the degree of latency as possible [29]. Thus, Oculus developers recommend certain system specifications, as given below, to minimize latency and improve graphics quality [32]:

Graphics Card	NVIDIA GTX 1060 / AMD Radeon RX 480 or greater
Alternative Graphics Card	NVIDIA GTX 970 / AMD Radeon R9 290 or greater
CPU	Intel i5-4590 / AMD Ryzen 5 1500X or greater

Memory	8GB+ RAM
Video Output	Compatible HDMI 1.3 video output
USB Ports	3x USB 3.0 ports, plus 1x USB 2.0 port
OS	Windows 7 SP1 64 bit or newer

Figure 1: Recommended system specifications for the Oculus Rift.

High processing power will allow the Rift to achieve the high frame rates needed to reduce latency. In addition, a powerful graphics card is needed to maintain the high resolution of the Oculus Rift and avoid VR sickness.

Search and rescue teleoperations can become challenging to navigate without a direct perception of the environment [33]. By using an HMD such as the Oculus to control a camera payload through head-tracking, situational awareness can be increased through a wider field of vision and the incorporation of depth perception [34]. Currently, two approaches exist to implement this method. The first is using a Free-Look Augmented Reality Display module to retrieve panoramic images taken from a spherical camera and to send these images to the HMD. The panoramic images are then stitched together and wrapped onto a sphere mesh, where images are split, one for each eye, to create a 3D image. However, this process is time consuming and any stitching errors that occur can cause disorientation, resulting in a trade-off between real-time data and image resolution [35]. The second method uses stereopsis, a process where two projections of an image are used to create depth perception, in which two stereo cameras can achieve a 3D effect from 2D imaging [34]. Head-tracking is achieved through the head teleoperation module, where the roll movement is used to control the camera. The angle

of head orientation determines the degree that the image must roll in order for the projected images to match the user position. A drawback to this method is the lack of a pan or tilt movement with head-tracking, resulting in a loss of visual information. This function can be achieved by adding a pan and tilt mounting to the stereo cameras and by correlating the yaw and pitch movements to the panning and tilting of the camera [36]. By improving upon this method, high image resolution and decreased latency can be maintained while adding depth perception, which will increase situational awareness for operators.

By presenting information that the user cannot see, AR visual overlays can increase an operator's situational awareness, which is useful for UAV operations [37]. A user's perception can be enhanced when viewing the real environment through the highlighting elements of interest, such as key landmarks or flight information from sensors [38]. The combination of sensor imagery with visual overlays reduces a user's scanning time while integrating information from disparate sources, allowing the user to concentrate on the task at hand [38].

Several issues become prevalent with using AR displays in regards to view management, the spatial layout of 2D objects [39]. The quantity of extra-sensory information displayed becomes a problem, as large amounts of information can cause displays to become cluttered [37]. Cluttered displays, often the result of unnecessary information, have the potential to overwhelm users, impacting the user's ability to complete a task [40]. Another aspect of view management is objective readability. In a study done by Azuma et. al., it was discovered that human subjects were able to read AR

labels fastest when the labels did not overlap, even if the placement was not ideal [39]. Thus, projected information must be appropriately arranged so that virtual objects do not intrude physical objects; otherwise, the overlapping of objects or the obscuring of background objects can cause objects to become impossible to read [39]. Lastly, cognitive tunneling causes another issue with AR displays and occurs when operators become so fixated on the 2D object from the overlay that they neglect to pay attention to the real environment [38]. Thus, the view management of the overlay in regards to positioning and visibility is extremely important in developing the AR display as unclear 2D objects may cause the user to become overloaded by the amount of visual information displayed. [39].

There are several view management strategies that can be applied in order to overcome AR display issues. Reducing the number of labels on the screen is one such strategy. The application of a filtering scheme, a system of prioritizing key information, so that information can be selected based on relevance to the task at hand, and unnecessary labels can be removed can remove clutter [41]. In addition to avoiding overlap between 2D objects, it is also important for the overlays to be placed so that it does not interfere with real world objects [41]. This can be avoided by placing 2D objects only in regions where there is less movement and interest [41]. To increase objective readability, overlays should not have any excessive movements that may distract the user [41]. In regards to textual 2D objects, features such as size, contrast, and font can be used to differentiate it from real-time surroundings [39]. The location of the 2D object must also be considered; for example, when considering labels, the farther the label is away

from the corresponding object, the longer it takes for the label to be read [39]. Other image enhancements can be used in order to improve visibility of overlays or highlight certain features, such as contrast, brightness, and transparency [37].

Several applications of AR displays have been used in previous research. One type of overlay that has been discussed is the virtual flag, which highlights key landmarks in the real environment using computer generated symbols [38]. The flag overlay is helpful during navigation due to its ability to pinpoint locations of interest and due to its simplicity which prevents cognitive tunneling [38]. One such project that uses the virtual flag incorporates an interface that is capable of identifying friendly, neutral, and hostile figures by recognizing icon shape and color [42]. It also offers an intuitive view of the operational environment that can identify landmarks, sun position, and other useful information about the surrounding environment [42]. This research also included development for a version for pilots, which provided real time information about the current flight space [42]. This technology could be modified for use in UAV control to identify points of interest for a search and rescue team, such as footprints or signs of habitation.

Another application of the AR display allows novice pilots to be able to learn controls and complete tasks in less time than using traditional methods. According to Goldiez et. al.'s comparison study on navigating mazes with AR assistance versus traditional methods, AR capabilities improved a subject's ability to navigate a maze with more transversal accuracy; however, the time required to complete the maze was not significantly improved ($p<0.05$) [27]. The results from this study would have been more

significant with more training for the AR users and fewer glitches in the software.

Overall, Goldiez et. al. conclude that AR shows promise in navigating through waypoints, but more research must be done before a significant correlation can be established [27]. A similar study conducted by Darken and Peterson also indicated some correlation and promise with respect to virtual reality guided interfaces improving navigation through waypoints [43]. This study aims to utilize an improved AR interface along with stereoscopic vision and useful flight information to improve the effectiveness of UAVs in search and rescue tasks.

Several studies have incorporated the Oculus with AR. These studies built their prototypes using the Unity engine, as it provides a flexible platform integrated with the Oculus [44, 45]. One method of creating the overlays takes advantage of Unity's ability to live stream videos to textures [44] and the software library Oculus Virtual Reality. The library allows for two cameras to render any digital content created in Unity and to create textures from the video connection data [44]. Another method uses a graphics library such as OpenGL to draw the overlays directly onto the video before sending it to the Oculus. Both of these libraries are possible avenues in creating effective overlays.

E. Data Transmission

Any UAV operation involving a human operator requires data transmission, as operator commands or video feeds must be sent to and received from the UAV. Both these tasks require communication to be consistent, accurate, and with minimum delay in order for the operator to maintain control and prevent VR sickness. For these reasons, a UAV being teleoperated by a user using an HMD requires two-way communication with

enough throughput to stream live video and less than 50ms total latency from user command to video response [46].

Wirelessly transmitting raw video at the resolution and frame rates desired for HMD use is infeasible because of its large data sizes. Therefore, the video must be compressed on the UAV before transmission and decompressed at the GCS after transmission. Data compression is the process of converting information from one format to another format which requires less bytes of data to store or transmit. The most effective video compression algorithms work by generating each frame of video by storing only a fraction of the frames as full images and storing the rest as a set of changes from the previous frame [47]. The frames stored as full images are called "key frames" because the rest of the frames are dependent on them. Current video compression software is capable of compressing and decompressing video in roughly 10ms [48], which is well under the threshold for VR sickness [46].

Teleoperation can pose challenges for the operator due to various factors. Video image quality may degrade over increased distance, obstacles, and signal interferences, resulting in poor spatial awareness. In a study, Van Erp and Padmos recommended the speed of transmission or frame rate (FR) to be at least 10 Hz to avoid poor video quality [49]. However, for navigation and tracking purposes, Thropp and Chen suggested to use higher FRs such as 15-16 Hz for more stable results [46]. Latency also poses an issue to teleoperation. A MacKenzie and Ware study demonstrates that error rates are increased by 64% when the latency is increased from 8.3 to 225ms. Supportingly, latencies as short as 300-320ms would also have a significant impact on the operator's tracking and spatial

awareness [49]. While other studies found that latency under 1s did not have any effect on the operator, but it did delay the operation. Besides delayed operations, latency can also cause VR sickness which is caused by the discrepancy between visual and sensory systems [49]. To minimize the problems caused by latency, a predictive display system is advised. Studies indicate that using predictive displays during teleoperation reduced the operation time by 17% [49].

F. Testing

The organization that is responsible for the safety of civil aviation in the United States is the Federal Aviation Administration (FAA). The major roles of the FAA include regulating developing systems for air traffic control and navigation, registering aircraft, and enforcing aircraft regulations and minimum standards [50]. With the recent increase in popularity of both hobby and military use of unmanned aerial systems (UAS), the FAA has created regulations specifically designed towards UASs and similar systems. In order to utilize a UAS for business purposes, the user must receive a Certificate of Waiver or Authorization (COA) from the Air Traffic Organization by submitting an online form for FAA approval [51]. This form covers a variety of topics, including but not limited to; aircraft model, operating altitudes, equipment on the vehicle, frequency usage, surveillance equipment, and flying locations [52]. The FAA passed a memorandum in May 2016 allowing students registered at accredited universities to fly in accordance with section 336 of the FAA Modernization and Reform Act (FMRA) for educational related purposes [53]. This interpretation change allowed the team to fly under section 336 regulations rather than acquiring a COA. Section 336 of the FMRA is a hobbyist

exemption that allows recreational flight provided that the UAV is flown in accordance within the rules set by nationwide community-based organizations, like the Academy of Model Aeronautics (AMA). UAVs flown under section 336 must weigh under 55 lbs, avoid interfering with manned aircraft, and must not be flown within five miles of an airport without prior consent.

The National Institute of Standards and Technology (NIST) is currently developing standardized tests to quantitatively evaluate aircraft and pilots in an effort to assist in the integration of small unmanned aircraft into the United States national airspace. These tests are split into three primary stages that increase in complexity. Elemental testing is designed to measure capabilities of the UAVs and pilots by completing specific tasks. These tests are constructed to identify and fix weaknesses within the system. The second stage evaluates mission proficiency by combining and sequencing the elemental tests in order to measure trade-offs of the system. The third and final stage embeds these systems into real scenarios in order to incorporate uncontrolled variables that may appear in real-world operations. This allows evaluators to evaluate the systems readiness.

At least five independent elemental tests are currently in development.The tests are designed to independently characterize the vehicle camera, platform performance, and operator ability. The first test is stationary and evaluates the payload camera's quality. The vehicle is placed on the takeoff platform. The payload camera is directed at a testing board, containing multiple symbols and characters, as shown in Figure 2. As the camera captures and streams video data of the testing board, the data is manually evaluated by

the vehicle operator. The data is analyzed to determine the camera's sensor acuity, in terms of visibility of the symbology on the board.

Figure 2: NIST testing board.

The second test evaluates the UAV's hovering and maneuvering capabilities. For this test, the vehicle takes off from a platform located in the center of four buckets. The pilot of the test UAV maneuvers the vehicle to align with a vertical bucket. Alignment is determined by viewing the bucket through the video stream captured by the vehicle's camera. If a centered circle with a letter inside is visible and legible, and the outer black ring is also fully visible, as shown in Figure 3, then the vehicle is considered aligned with that bucket. Then, while maintaining alignment with the first bucket, the vehicle must also align with the opposite 45-degree bucket. This is repeated for each of the four

vertical buckets around the takeoff platform and then repeated again for the larger test stands. The primary data collected from this test is the required time for completion and the number of collisions with test equipment or the ground, if they occur.

Figure 3: NIST testing bucket with letter inside.

The third test is very similar to the second, but rather than aligning the UAV with the buckets, the pilot maneuvers the UAV such that a smooth circle can be made around the center apparatus. The pilot must also check their alignment every 90 degrees of rotation using the central and radial test stand buckets. This test examines the pilot's ability to correctly position the UAV about some point of interest. The fourth test is a vertical positioning test where the UAV must align itself with buckets that are mounted horizontally on a vertical pole at differing heights. The pilot attempts to capture each bucket and identify its alphabetical letter.

The last test is a maneuverability test where the pilot navigates the UAV in a figure eight pattern around two colored poles of two gates while remaining under a defined limit. This test evaluates the UAV's ability to maneuver in confined spaces. These standardized test procedures currently in development will help govern the future of small UAVs; therefore, similar testing metrics should be considered for the proposed

system to determine the capabilities and benefits of the system, along with highlighting areas of improvement.

G. Conclusion

The surveyed literature discusses current SAR-specific UAV capabilities, the characteristics of monoscopic versus stereoscopic vision, the current standards of AR and VR interfaces, the data transmission requirements, and finally, the testing of the developed user interface. As UAVs are aerial vehicles that can be controlled from a distance, they offer unique advantages in managing search and rescue operations, such as reduced danger to searchers and increased search efficiency. Based on the relationship among all of the factors described in the literature, we propose the following hypotheses: stereoscopic vision will improve UAV operations, stereoscopic vision will significantly affect UAV operator visualization, and that a AR and VR interface will improve upon existing search and rescue methods. These hypotheses agree with the team's goals and supports the concept of the system the team wishes to create. By utilizing stereoscopic vision to improve UAV operation and operator visualization, the team will be able to create a UAV system that allows search and rescue operators to locate victims more easily and efficiently while reducing the risk to human lives.

III. Methodology

A. Introduction

Team ARM IT developed an AR and VR interface to control the sensory payload of a UAV. The research was divided into three components: payload, platform, and GCS. The payload component is a hardware component mounted on the drone and provides

high-resolution stereoscopic vision for the UAV operator. The UAV platform consists of the vehicle itself and will act as a navigation and transportation unit, allowing the operator to remotely interact with the environment. The GCS consists of a computer with the appropriate software and processing power, which runs the VR user interface that controls the payload and displays the information from the platform on a HMD. This interface is designed to display on an Oculus VR headset, which the GCS works in conjunction with.

The research questions that the team looked to answer over the course of this project are:

1. How does stereoscopic vision improve UAV operations?
2. How does utilizing VR as the delivery method for the video feed from the sensory payload affect how the operator visualizes the search and rescue environment?
3. How does a VR interface that controls a sensory payload of a UAV in order to conduct search and rescue improve on pre-existing search and rescue methods?

B. Preliminary Cylinder Test: Stereoscopic versus Monoscopic

In order to determine the benefits and limitations of stereoscopic vision in comparison to monoscopic vision, a preliminary depth test was conducted. This test assesses a subject's ability to determine the relative distance from the viewpoint of two cylinders. The test was conducted by having a subject align two similarly shaped and colored cylinders spaced a fixed distance apart in a 3D virtual environment. The test was assessed twice, once with a flat monitor to test the subject's ability using monoscopic vision and once with an Oculus Rift to test their ability using stereoscopic vision. The error between the subject's positioning of the cylinder and the positioning at which both

cylinders were at the same depth was then analyzed to determine if one vision type allowed for an increased depth perception when compared with the other.

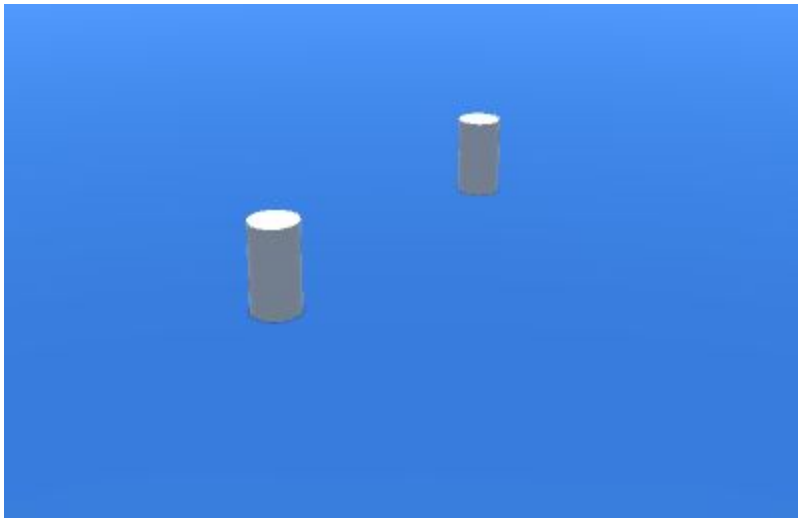

Figure 4: Preliminary cylinder test.

C. System Overview

The system consists of two main parts: the payload aboard the UAV and the GCS. The payload contains a stereoscopic gimbal system housing two cameras. The pilot operates the gimbal system from the GCS through an Oculus Rift HMD. The pilot's head rotation data is obtained from the Oculus Rift and is transmitted to the UAV; the gimbal rotates in accordance to the received data to mimic the pilot's head movements. Video data from the cameras on the payload is transmitted to the HMD, enabling the pilot to see from the UAV's perspective through VR. The video streamed to the GCS is augmented with overlays of flight and mission data.

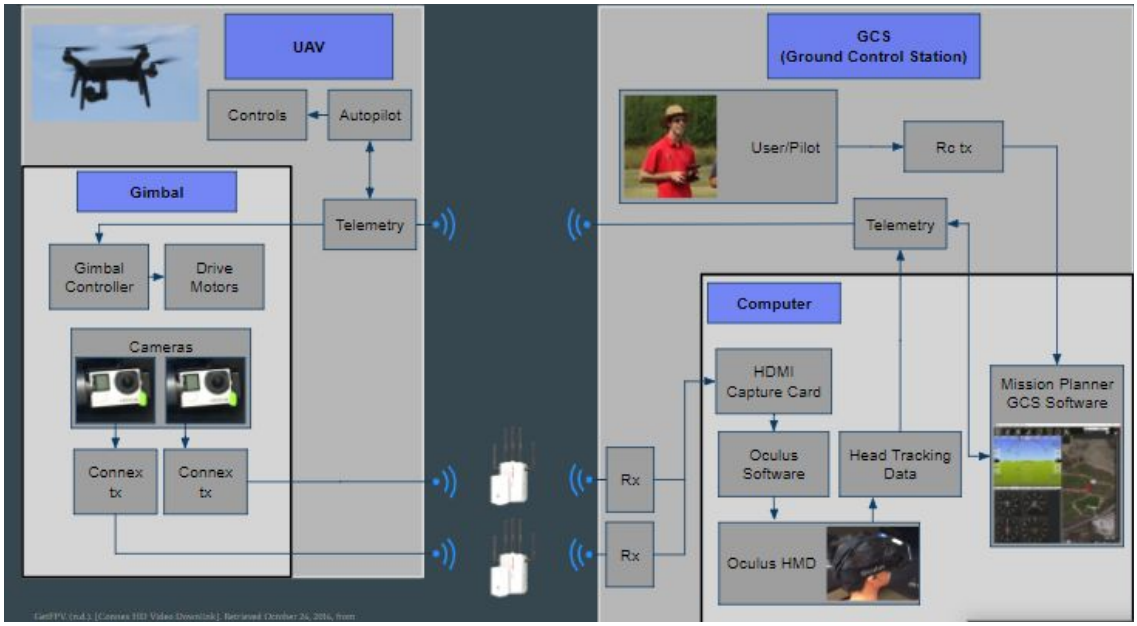

Figure 5: System architecture

D. Payload

The payload component provided high-resolution stereoscopic vision for the UAV operator. In order to achieve stereoscopic vision for the UAV operator, Team ARM IT developed a custom gimbal design as part of the UAV payload, incorporating a two-camera arrangement. This design also allowed for better situational awareness for the UAV operator. The head movements of the ground operator wearing the Oculus headset synchronized with the camera movements on the UAV, allowing the operator to look around the UAV as though their point of view was from the UAV itself. These design choices for the custom gimbal were made to obtain better situational awareness in order to improve on existing SAR methods.

Two GoPro HERO4 Black cameras were used to simulate a single stereoscopic camera. The camera was chosen for its high definition 1080p resolution at 120 frames per

second (FPS). The resolution and framerate of the camera were necessary to match the input requirements of the Oculus, and to combat the effects of VR sickness [31, 54]. This allowed for a clear video stream from the UAV to the HMD, which is required in SAR situations to distinguish environmental features [55]. Stereoscopic vision was achieved by positioning two cameras adjacently on the UAV and then transmitting the two video feeds from the cameras to the HMD. The IAD, or the distance separating the centers of the two cameras, must closely match the user's IPD, or the distance between the user's pupils, in order to mimic stereoscopic vision. As human IPD varies from 52mm to 78mm, the IAD of the cameras can be adjusted to account for this variance [25]. For an ideal calibration, the user's head will be positioned in the Frankfurt plane, an anthropometric head position, and the distance between the subject's supraorbital foramen will be measured using anthropometric calipers positioned parallel to the ground. The camera spacing was adjusted before flight to match the distance measured by the calipers. After adjustment, the payload was recalibrated to ensure stereoscopic vision was achieved after being mounted onto the custom gimbal, to be discussed next.

The custom three-axis gimbal was designed by the team in order to suit the team's need for a gimbal that supports stereoscopic vision. Having previously selected the cameras, the next design choice was the motors for the gimbal. The motors were crucial to creating a realistic experience of matching the camera motion to the user's head movements. The cameras mounted on the gimbal must allow rotational freedom to pan, tilt, and roll in order to mimic natural head movements. With a dual inertial movement unit (IMU) setup, where one IMU is placed on the cameras, and one IMU is placed on the

gimbal frame, the gimbal was able to have full 360-degree rotation. This structure, as opposed to using only a singular IMU, prevented gimbal lock, a condition where two motors attempt to control the same axis and cause uncontrollable oscillations.

In order to further increase the accuracy of the camera's movements in relation to the users, the team opted for motors that included encoders. Encoders allow for greater precision and reliability while stabilizing the cameras. This feedback loop is due in part to the encoder's ability to track and measure the motor shaft speed and positioning, which was necessary to obtaining precise control over the gimbal's actions. However, issues were encountered while incorporating these components into the gimbal. Each axis of the gimbal performs as expected separately and in combination with any other single axis, but when all three axes of stabilization are activated, uncontrolled oscillations occur on the pitch axis at angles of plus or minus 20 degrees of base platform pitch deflection. This issue remains unresolved at this stage of the gimbal development.

In addition, the use of brushless motors allowed for higher precision when compared the alternative of servo motor driven gimbals. Brushless motors have no direct mechanical link along their rotation axis, which allows the gimbal to use inertia to its benefit. Even without power, the inertia of the cameras on the end of the gimbal will cause them to tend to stay pointed in the same direction if the gimbal is moved or rotated. In addition, the gimbal controller incorporate gyros and accelerometers in order to precisely measure the shifts in the payload. Having precise movements also helps to reduce any motion sickness from using a virtual reality headset due to its smoother operations, and thus more closely replicated the user's head movements in real life. The

disadvantages in using brushless motors only lie with its difficulty to balance, which can be compensated for in the overall gimbal design.

Throughout the gimbal design process, the goal was to optimize the compactness and balance of the gimbal. Compactness ensured that the payload could easily attach to the UAV itself and not hinder the UAV's maneuverability. It was also more cost-efficient as it required fewer materials and parts to produce. Balance was also a crucial part to the gimbal design in order to maximize stability of the payload on the UAV, reduce strain on the brushless motors, and more accurately replicate the user's movements. Many design iterations and prototypes were created in order to best meet these requirements. Hence, the gimbal was constructed from 3D-printing using parts designed using the computer-aided design (CAD) programs Autodesk Inventor and Fusion 360. Using 3D-printing sped up the prototyping process, as designs were able to be relatively quickly manufactured, tested, and then reprinted if necessary. In addition, it allowed for greater design freedom and customizations that were necessary to produce the best possible gimbal.

Over the process of building and refining the gimbal, the team went through several design iterations. First, the team designed a gimbal with a typical single-camera configuration from which to begin modifications. This basic setup allowed the team to be able to get a feel for future changes and how to best proceed in developing the stereoscopic gimbal. The team was able to examine how the 3D-printed single-camera gimbal operated, and in particular, how the camera could fit into the gimbal and rotate with smooth operation.

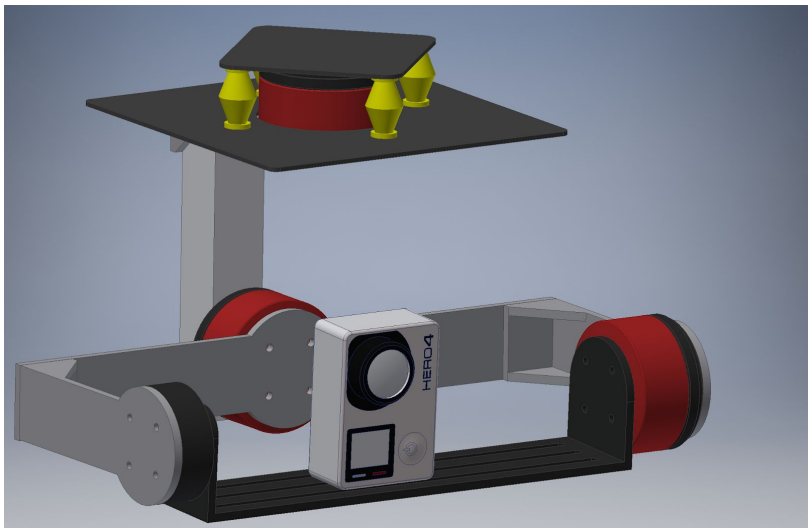

Figure 6: Custom-built gimbal with a single-camera configuration.

The second iteration, which was an elongated and enlarged version of the single-camera gimbal configuration, included the additions of the second camera. This was the first step into achieving the stereoscopic gimbal. However, adding the second camera introduced many different design issues, such as balance and compactness, that were not encountered with a singular camera. This was in part due to the difficulty in using the small space efficiently. These design fixes are explained in the later design configurations.

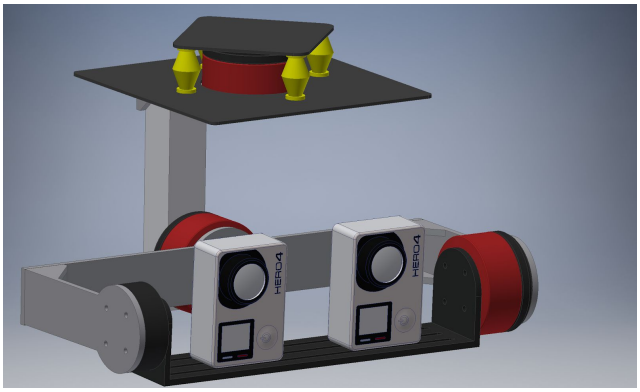

Figure 7: Custom-built stereoscopic gimbal design iteration 1

The next iterations were focused on downsizing the number of parts used while retaining functionality. The simplification of part counts on the gimbal consequently led to better prints and a cleaner, more compact design. Due to the modular design of the system, having a more condensed gimbal design enables it to be paired easily with a variety of different UAV systems.

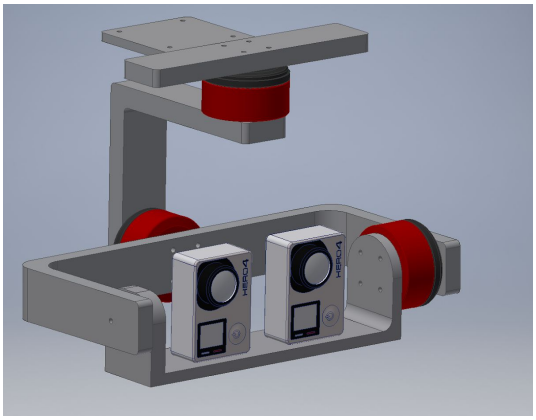

Figure 8: Custom-built stereoscopic gimbal design iteration 2.

The main issue with the first two designs was balance versus centered rotation. In order to have the gimbal have neutral balance, such that the gimbal could rotate to any point in space while remaining stationary, the camera(s) must be moved to the side of the platform opposite the pitch motor to offset its weight. However, moving the camera(s) to the side means that the roll movements of the camera(s) would occur off-center of rotation, which creates undesirable vertical motion of the camera relative to the object of interest. As the distance to the object is reduced, these motions will become more obvious to the operator. Throughout these iterations, the team discovered that positioning the motor in the center, with the two cameras placed on either side, was the best method to achieve proper balance while maintaining compactness. While the yaw axis motor and

roll axis motor remain in the relative same position, the third iteration placed the motor in the center of the cameras. In addition, in previous iterations, more space was provided between the frame, motors, and camera. The team found that the extra space was unnecessary and hindered the compactness of the design. In this next design iteration, the spacing was decreased. Later design iterations would tweak the spacing in order to allow full movement of the gimbal during rotation and allow the cameras to easily fit onto the frame.

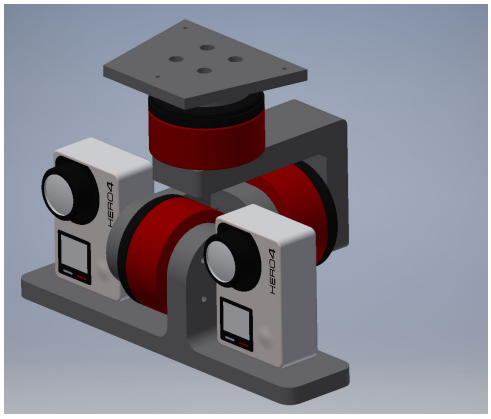

Figure 9: Custom-built stereoscopic gimbal design iteration 3

In addition, the team tested the gimbal after each 3D-print for two other factors: tolerance and durability. The gimbal was tested for correct tolerance, to ensure that the design did not impede movement from the motor once it was mounted onto the gimbal. In addition, the gimbal was tested for its durability in order to guarantee that none of its components would break when used. The team discovered that the 3D printing material also played a part in the gimbals' durability. The team initially chose to use ABS (Acrylonitrile Butadiene Styrene) materials, which has higher ductility than PLA (Polylactic Acid), which is more brittle. However, the quality of the parts produced with ABS was

inconsistent and often shattered along the print layers under stress. Ultimately, the team designed a gimbal using PLA parts that satisfied the requirements necessary for a successful SAR mission: compactness, balance, durability, and tolerance. The final gimbal design and rendering are presented in Figure 10.

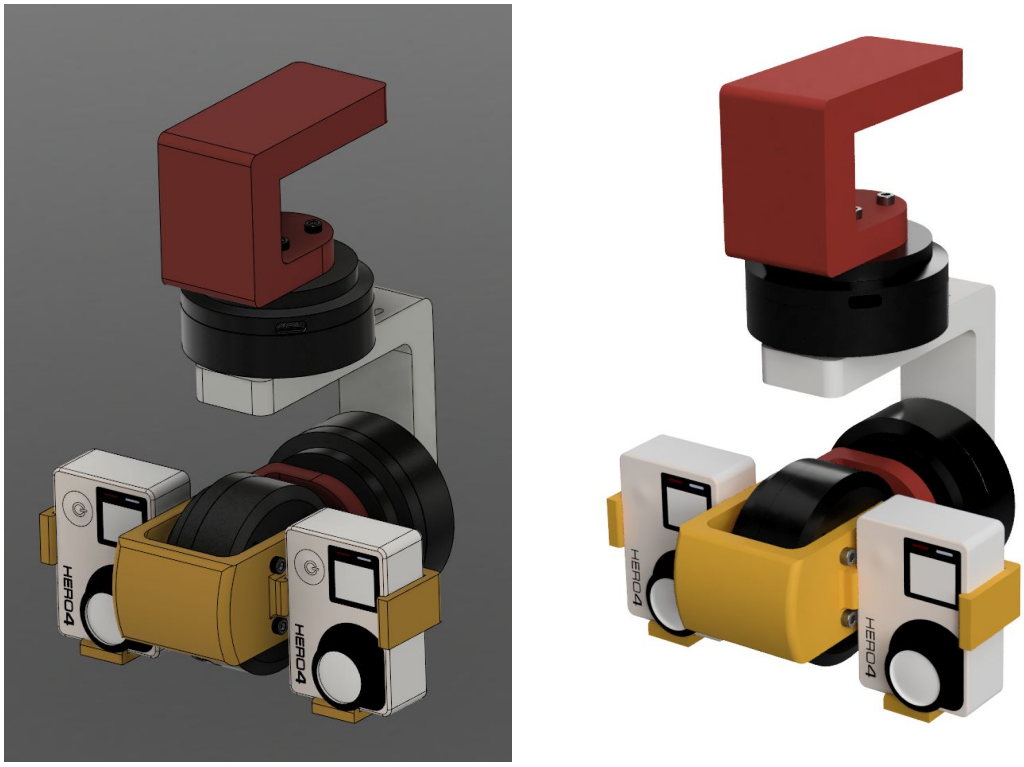

Figure 10: Final gimbal design (left), final gimbal rendering (right).

The other payload components of the UAV included the batteries, transmission (Tx), and reception (Rx) equipment. Two separate rechargeable battery packs are used to power the gimbal motors and transmission equipment since the two have different input voltage requirements. Purchase of the cameras includes rechargeable batteries, so a power supply for them is not needed. The gimbal controller requires an input voltage of around 12 V. The transmission equipment on the UAV has an input voltage range from 6 to 25V. Two

11.1V 3s Lithium-ion polymer (LiPo) battery packs will be used due to their high storage capacity to weight ratio. The transmission equipment and power components will be assembled according to Figure 11.

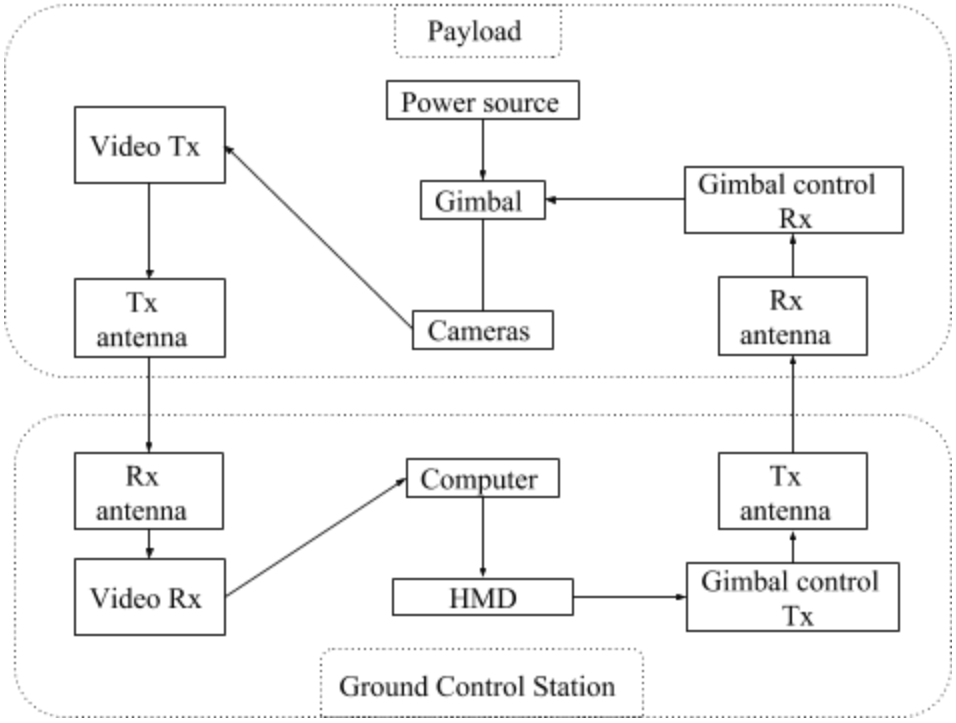

Figure 11: Transmission and power diagram.

After assembling the camera setup and transmission equipment on the UAV, communication will be established between the cameras and the HMD. The reception of this data as well as displaying this video data on the HMD screens will be discussed in the following sections.

E. Computer Setup

Following the system specifications outlined in the literature review (Figure 1), the team built a total of three computers that matched or went beyond the recommended system requirements. All three computers were built to optimize and support the high

demands placed on Oculus operations, including the minimization of VR sickness. Thus, computer parts were chosen in order to maximize processing power. There were two types of computers assembled in order to fit our needs. The first computer, built in the initial stages of the project, was used to develop the Gimbal-Computer pairing needed in the project, as further detailed in the next section of the methodology. Therefore, the only constraint was the need for a powerful graphics card in order to run the Oculus successfully. In particular, an NVIDIA graphics card was needed in order to support the CUDA libraries that were used in the Gimbal-Computer pairing. The CPU and other hardware were chosen based on its known history of good performance and cost-effectiveness. The details on the particular CPU, RAM, and graphics card are shown below, along with a figure of the completed setup, with a full parts list located in Appendix A.

CPU	Intel - Core i7-4770 3.4GHz Quad-Core Processor
RAM	Corsair - Vengeance Pro 16GB (2 x 8GB) DDR3-1866 Memory
Video Card	EVGA - GeForce GTX 980 Ti 6GB Superclocked+ ACX 2.0+ Video Card

Figure 12: Partial computer parts list.

Figure 13: Assembled computer setup

The second type of computer built was reserved for testing stations needed for the flight simulation tests, which are described in later sections of the methodology. Multiple testing stations were built to speed up the testing process, allowing several participants to be tested at once. While the first computer was built for cost-efficiency, the second set of computers was created in order to run high-resolution simulations; the result being that processing power becomes a greater factor than in the previous use case. The CPU was chosen for its power, using a 16-core processor in comparison to the first computer's quad-core processor. In addition, because the flight simulation was developed in UnReal Engine, the video card chosen was one that was known to work well with this development engine. Based off of these two factors, the rest of the hardware chosen was in compatibility with the CPU and video card. The details on the particular CPU, RAM, and graphics card for the testing stations are shown below, with a full parts list located in Appendix A.

CPU	AMD - Threadripper 1950X 3.4GHz 16-Core Processor
RAM	32GB Corsair Vengeance LPX 3200MHz
Video Card	AMD - Vega Frontier Edition 16GB Frontier Edition Video Card

Figure 14: Partial computer parts list for the testing stations.

F. Gimbal and Computer Pairing

The next step in the creation of the camera gimbal is to pair it with the GCS, such that the movement of the user's head synchronizes with the movement of the cameras onboard the gimbal. This synchronization will allow for the natural movement of the user to translate to their view of the UAV, despite its teleoperation. Completing this pairing will allow for improved situational awareness due to the stereoscopic vision from the two-camera custom gimbal. In turn, the more realistic perception of the UAV's surroundings will improve the sense of direction for the operator as well as ease the learning curve for new users operating the UAV.

An overview of the system is as follows. The system takes in wirelessly communicated, real-time video feed from two cameras on the UAV. This set of data is then merged into a stereoscopic video display for the user. Simultaneously, the system will obtain head-motion tracking data from the VR headset and wirelessly send it to the UAV for the purpose of controlling the motion of the gimbal on the UAV. The gimbal will then control the positioning of the two cameras on the UAV with the transferred data.

There are two main focuses for the system to operate successfully. The first is to adjust the video to mimic natural stereopsis and stream them to the Oculus Rift VR headset. To this end, the two videos from each camera are warped with a barrel distortion to counterbalance the pincushion effect caused by the VR headset. This allows the inherent image magnification from increasing distances along the optical axis to be neutralized and give a more natural perception. After this transformation is applied, the video is then displayed on the headset. At the beginning of the code development, the team used the ZED camera for streaming, which is known for its high-definition 3D video, synchronized left-and-right video streams, and ability for depth-sensing [56]. The ZED camera was a useful beginning development tool as it came with many pre-built libraries that make the camera easy to use, including starting code to stream the ZED to the Oculus. However, for SAR applications, using the ZED camera was not feasible due to its slow streaming speed and its bulkiness. Instead, two GoPros were used in order to achieve high quality video along with high streaming rates. By modifying the pre-existing ZED to Oculus code, the GoPro videos were able to be displayed on the Oculus headset. This was achieved by replacing the video feed from the ZED to come from the GoPros instead. In addition, the appropriate video card driver must be installed. For the program to run successfully, the Oculus must be running at the time of application start. The Oculus has a sensor at the top of the display that detects when a person is wearing the headset. Unless this sensor is activated, nothing can be displayed on the oculus. When testing, the sensor should be covered by either a finger or some adhesive.

The code to stream video to the Oculus headset, which includes the custom barrel distortion program, was developed in C++ in Visual Studios 2015 on Windows 10, and eventually built into an executable file. The libraries and platforms needed to compile this project include OpenCV (for real-time computer vision), OpenGL (for graphics rendering), Oculus SDK (for Oculus development), and CUDA 8 (for general purpose processing on graphics processing units). Although currently the most recent version of the CUDA platform is CUDA 9, the program is unable to run in this version as certain libraries are not able to be found, due to the way the libraries are split. In order to solve this problem, the team was able to merge all the separate libraries into one library, but also decided to revert back to the previous version. In addition, when working with the ZED camera in the initial development stages, the team found that the ZED SDK may need to be re-installed in the event that program is unable to find the ZED (specifically, the camera.hpp file). When working with the GoPro cameras, many linking errors were encountered and solved. For a full detailed list on the solutions to these debugging issues, see Appendix B. Additionally, the code to create the camera to Oculus streaming can be found in Appendix C.

The second main focus is to mimic natural head rotations with the gimbal system. The system uses the Oculus Rift as the VR headset to link to the gimbal attached to the UAV. By utilizing the Oculus, the system is able to track the movement and orientation of the wearer's head, as shown in the Figure 15. The Oculus positions must then be mapped to the corresponding gimbal positions.

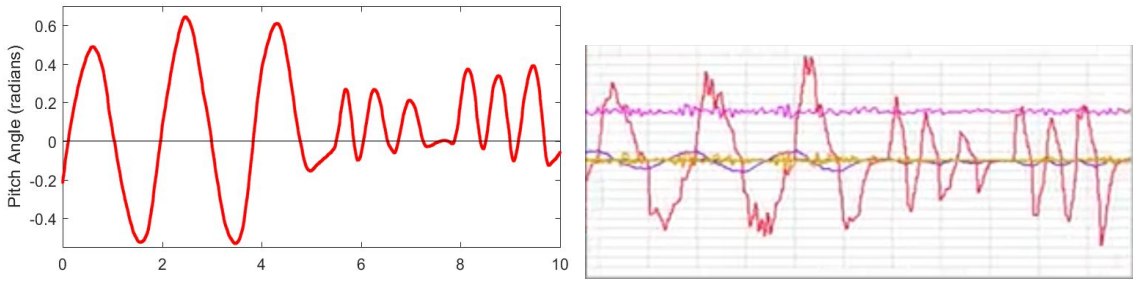

Figure 15: The mapping of the Oculus pitch output (left) to gimbal motor pitch output (right).

The Oculus outputs this orientation as a 4-tuple of Quaternion angles, a convenient method of representing spatial rotations in three dimensions. However, in order for these angles to be used by the gimbal controllers on the UAV, the Quaternion angles must be converted into Euler angles, which give orientation using a fixed coordinate section and thus can be directly translated into roll, pitch, and yaw rotations [57], as shown in Figure 16.

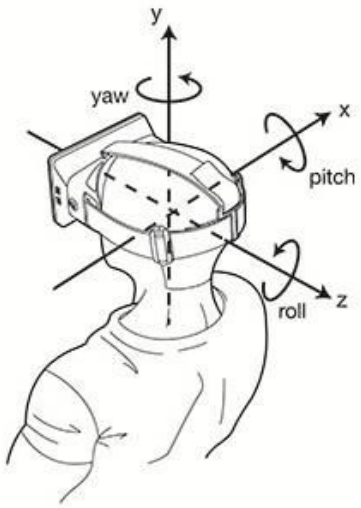

Figure 16: Euler angle diagram with yaw, pitch, roll axes.

This translation is handled within the software program, developed in Python, and can be determined by the following formulas, where q_0 - q_4 represent quaternions:

$$\begin{bmatrix} \phi \\ \theta \\ \psi \end{bmatrix} = \begin{bmatrix} \arctan\frac{2(q_0 q_1 + q_2 q_3)}{1-2(q_1^2+q_2^2)} \\ \arcsin(2(q_0 q_2 - q_3 q_1)) \\ \arctan\frac{2(q_0 q_3 + q_1 q_2)}{1-2(q_2^2+q_3^2)} \end{bmatrix}$$

Figure 17: Quaternion angles to Eulerian angles translation.

A second step is required is required for gimbal controller operation, in which the Euler angles are mapped to Pulse-Width Modulation (PWM) values using linear interpolation, as given below, where θ takes on the roll, pitch, and yaw angle values in radians:

$$PWM = \frac{800}{\pi}\theta + 1500$$

Figure 18: Linear interpolation.

The mapping corresponds the Euler angle $-\pi/2$ to the minimum value 1100, and the Euler angle $\pi/2$ to the maximum value 1900. These PWM values are fed directly into the GCS via wireless communication through the Micro Air Vehicle Link (MAVLink), which is already included as a subsystem of the UAV itself. Thus, the system does not require any additional transmission equipment outside of what the vehicle itself includes for the gimbal control. Commands to the gimbal controller are sent using functions from the built-in MAVLink API. The PWM pulses can then be used by the gimbal controllers to rotate the motors to the desired angle, matching the user's head movements with the camera. To ensure a balanced system, the speed of the gimbal movement must be capped

at a maximum speed. This speed can be adjusted to match the performance of the gimbal controllers, such that the gimbal can operate smoothly. The software developed by the team relays the PWM values for the roll, pitch, and yaw of the user's head movements every 10 milliseconds in order to achieve the natural head movements. In addition, because the system developed is compatible with commonly used GCS software and gimbal controllers, the system is simple to use with already-existing UAS. The code to synchronize and move the gimbal can be found in Appendix C.

The system setup for this project can be completed with these steps:

Hardware setup:

1. Make sure the Oculus and its sensors are connected to the GCS via USB 3.0 ports.
2. Make sure the GoPros and the batteries are all fully charged.
3. Connect the GCS Connex to a power supply and plug in batteries to the gimbal Connex.
4. Connect the GCS Connex to the video capture card, then turn on both GCS Connex and gimbal Connex.
5. Plug the gimbal Connex to the GoPros using ribbon wires. Note: Do **not** use regular wires, as those will interfere with gimbal control operations).
6. Plug the batteries into the motor controller and MAVLink.
7. Begin software side of setup.

Software Setup:

1. Note that the ordering of these setup steps is **very** important.
2. Use the *webcam_to_oculus* executable to start display of GoPros to Oculus.

3. Make sure that someone is wearing the Oculus.
4. After the video stream begins, execute the python code that connects gimbal to GCS.
5. System should be fully operational within a few seconds.
6. If there are problems with the display, debug any errors in the C++ code.
7. If there are problems with the gimbal, connect the gimbal controller to the GCS and debug using the SimpleBGC software. (While the python code will not likely be an issue, check the angles.txt for errors in the output).

G. Oculus Streaming

A VR display using live video feed requires a data link with high bandwidth and low latency to provide high enough quality video to prevent VR sickness. In addition to being sufficiently low, the latency must be consistent within the operating range. For one video feed with the required 60 frames per second and 1080p resolution, the data link must sustain at least 12000 kbps of bandwidth with less than 50ms of total latency. For a stereoscopic display using a two monoscopic camera feed, the required bandwidth doubles to 24000 kbps.

The transmission hardware used to achieve these speeds is the Connex video transmitter [58]. The Connex can transmit video at the required 60fps and 1080p at a range of up to 500m. Additionally, the latency of the Connex is less than 1ms, which is the lowest latency of any transmitter on the market. When parts for the system were being selected in February 2016, this was the best video transmitter available in the <$1500 price range. The system used two Connex transmitters to send the left and right video feeds separately.

The flow of the video transmission system begins with the two GoPro cameras mounted on the gimbal. Each of these cameras is connected to a separate Connex air unit through the built-in HDMI port. The cameras capture the video and send it to the Connex for transmission. The Connex air units send the video feed wirelessly to the Connex ground units using the 5.8 GHz radio frequency. The Connex ground units then receive the video transmission and send it to the GCS via a dual-input video capture card. After the GCS receives the video, the video feeds are distorted to fit the Oculus Rift's display using a custom barrel distortion program written in C++. The source code for transmission can be viewed in Appendix C. The distorted video feeds are then displayed to the user through the Oculus Rift. This process happens continuously for the duration of the flight.

H. Stereoscopic Overlays

While development of a virtual reality system for seeing through the eyes of the drone offers many benefits in terms of depth perception, it presents several issues in terms of the developer's ability to present the pilot with flight information. Typical drones are able to provide the user with important flight data such as altitude and signal strength through a simple graphical user interface on a screen. Furthermore, the operator is able to observe the drone from a third person perspective, which is far better at providing information about the height of the drone above the ground and distance from the user. The importance of these pieces of data to any drone pilot necessitates the development of another method for providing a pilot of the VR system with flight data.

Overlays in virtual reality have several requirements that make them less easily implemented than traditional overlays. First and foremost, there are two screens that have to be provided with the same information. While simple enough at first, the two overlays must be offset appropriately to provide the semblance of distance, yet not so far apart that the overlays appear to be mere inches from the user's eyes. Thus, any overlay must be designed in three dimensions. According to Oculus Rift online documentation, any important information must be placed within the middle third of the screen, and appear around 2 meters away from the user. This provides even further constraints in that the data must be centrally located, yet also not interfere with the user's vision of the camera feed.

In keeping with the constraints listed above, an overlay for the camera feed to the Oculus Rift was developed to provide the user with flight information. The overlay itself was programmed using OpenCV to draw the necessary shapes and text. Each video feed has the overlay drawn over the incoming images, which are then provided to the Oculus Rift. The overlay takes the shape of a rectangular box in the upper part of the screen, with readings for drone altitude, flight speed, signal strength, battery life. The center of this box has a circular compass for telling the orientation of the drone while in flight. A sample sketch of this overlay layout is in Figure 19.

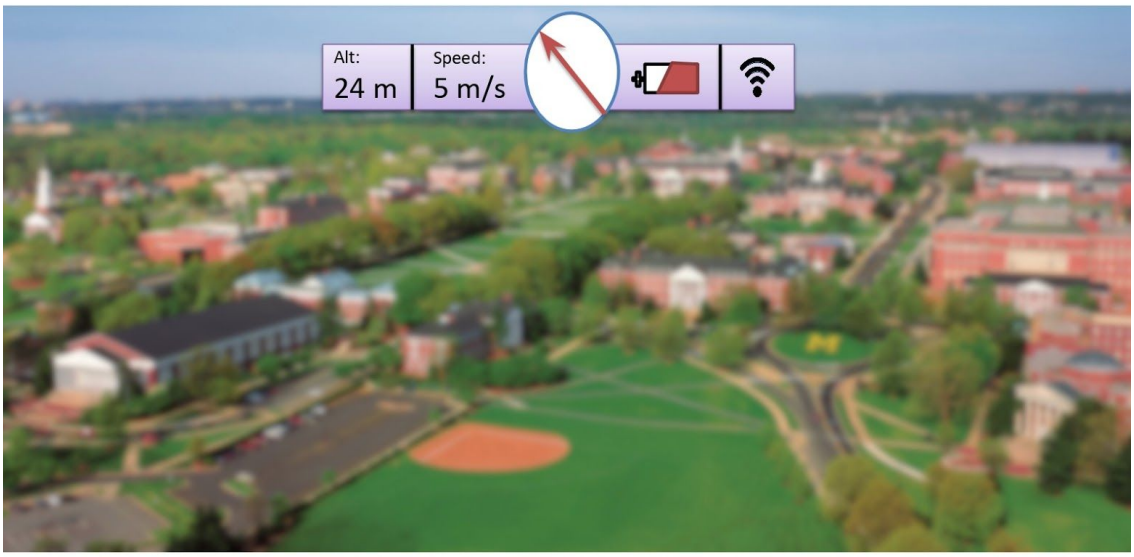

Figure 19: A sketch of the overlay system developed over a sample background.

The data for these fields can be obtained from most autopilot systems as a standard feature. By importing the data from the autopilot system in real time, the overlays can be updated to reflect actual flight data of the drone.

Live stereoscopic facial detection and upper body detection relies on the pre-trained OpenCV classifier called the Haar cascade. The Haar cascade classifier is trained based on Haar-like features, which are digital image features commonly used in image recognition. Figure 20 shows several examples of Haar-like features.

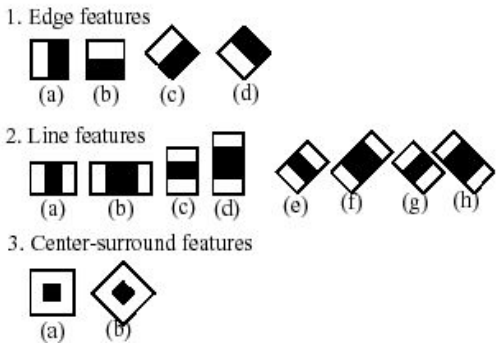

Figure 20: Haar-like features.

The Haar cascade comes with variety of detection options when it comes to image recognition, enabling more options for overlays. However, over the course of overlay development, the team noted that having more cascades degrades the frame rate of the video feed and hence increases the likelihood of VR sickness. Utilizing newer graphics processing units (GPUs) and techniques like parallel computing can help speed up the computations and lead to a smoother video feed. Facial detection was only nominally incorporated into the team's system, but future prototypes could compare faces recognized with this technology to a database of missing persons to identify victims. This is only one example of the possibilities involved with incorporating facial detection into the visual overlay system.

The framework for importing this live data and facial detection has been developed to allow any drone system to use this system. Due to the variety of potential systems for drones, this system integration was purposefully left for future users of this prototype to implement in a manner that would suit their system. The figure below shows the overlays implemented without real-time data, the initial step for future prototypes.

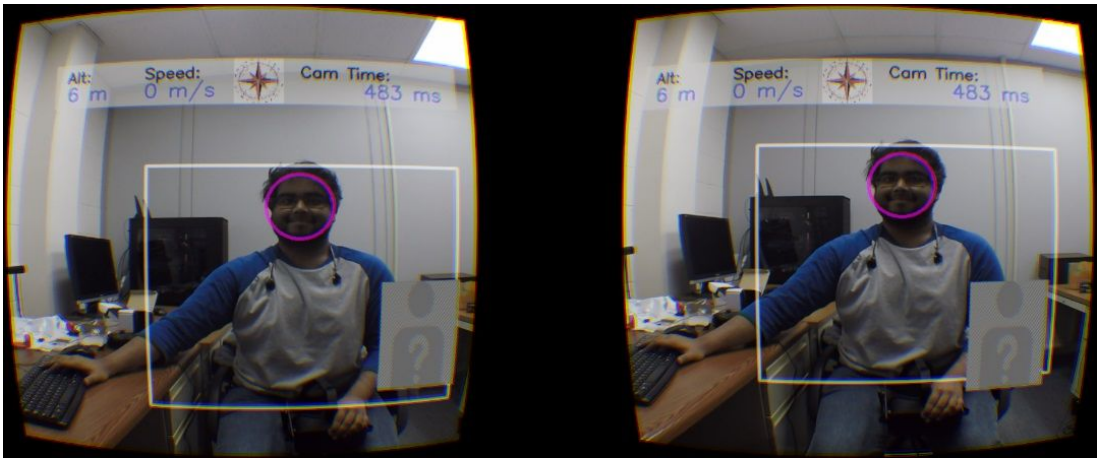

Figure 21: Augmented overlays and facial recognition on stereo camera system.

I. Initial Communications Testing

In order to ensure proper operation of the UAV, it is imperative to know the limitations of the communication hardware. If the UAV exceeds the maximum safe operating distance of the Connex, the HMD will be rendered useless and safe operation of the UAV will not be possible. Thus, an initial communications test was performed in order to verify the range capabilities of the Connex video transmission system.

The test consisted of two parts. First, the Connex video transmission was tested to ensure the correct assembly and proper operation of the system. This test involved powering the system and verifying a video stream was passed from the GoPros through the Connex transmission system to the ground station monitor. Second, the system was tested to determine its range limitations. During this test, the GCS Connex receiver was connected to a monitor and held stationary in an outdoor setting. The UAV Connex transmitter was connected to the two GoPros which had a video feed streaming to the GCS monitor. The UAV transmitter was then moved at incremental distances away from the receiver until a noticeable lag occured in the video data. The test was continued until a complete loss of signal occurred. The results from this test helped determine the range capabilities of the team's system. The full testing procedures can be found in Appendix F.

J. Flight Simulation Tests

The team developed a flight simulation in order to test the research question of how stereoscopic vision can improve UAV operations, without the use of a physical UAV. The use of a simulation allows for a more controlled environment for testing. Participants were asked to take a series of tests in a virtual environment with a simulated

UAV. The sample group consisted of 18 participants enrolled in the University of Maryland, College Park. In order to test on human subjects, the team had to receive approval from the Institutional Review Board (IRB) located in the University of Maryland, College Park. Approval for this project was expedited, because the team's study was considered low risk for participants. Participants used both a regular computer monitor to simulate monoscopic vision and an Oculus Rift virtual reality headset to represent stereoscopic vision in order to compare the two types of visions and the manner in which it affected the participant's ability to complete the test. Both the computer monitor and the Oculus Rift are operated in the same resolution of 1080p to establish equal testing conditions across both platforms. Before the tests, participants noted their UAV experience in hours and thus placed themselves into one of three categories: no experience, beginner experience, and advanced experience. In addition, to reduce biases in tests due to unfamiliarity with the system set-up, all participants underwent a short training period for acclimatization.

The flight simulation was divided into two tests. The first test was a movement test to determine the effect of stereoscopic vision on how the participant handled the UAV and if it increased their overall level of perception of the environment. The second test was a search and rescue test, which was conducted in a virtual environment as similar as possible to a real search and rescue scenario. This test was used to determine whether stereoscopic vision improved the operator's ability to search an area from an aerial vehicle.

The movement test and the search and rescue test were built using the Unreal Engine version 4.16.3. This engine was chosen primarily due to the existing compatibility with an air simulation plugin, thus reducing development time for the simulation levels. No proprietary assets were used in the development of either level. The humanoid figures are 1.5 meters tall, which are placed into a realistically scaled environment. The figures have a main body color of yellow, with a colored circle on the figure's chest. Each search and rescue level consisted of 15 humanoid figures dispersed throughout the map with unique chest colors.

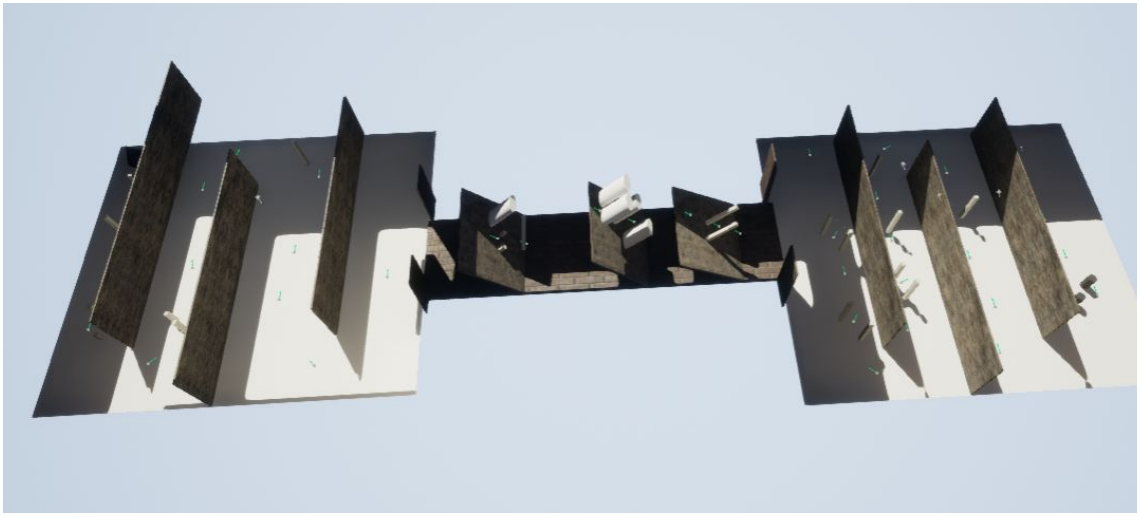

Figure 22: Movement test.

Figure 23: Search and rescue test.

The goal of the movement test was to analyze how stereoscopic vision affected the manner in which an operator handled the UAV and how this translated to collisions with the environment. The hypothesis was that if users were able to utilize stereoscopic vision to perceive depth more effectively and thus navigate better in their environment, this would translate to better UAV operation outside of the simulation as well. In the movement test, users were instructed to fly through a series of rings placed in an aerial obstacle course, which grew progressively more difficult over the duration of the course. Users were given five minutes to complete the course by reaching the black cone at the end of the area. Many of the obstacles consisted of walls, pillars, and inclines. Participants flew the course twice, once in monoscopic and once in stereoscopic vision, and the order in which they took the course was randomized in a controlled manner to ensure that approximately half of the participants flew the stereoscopic version first and

half flew the monoscopic version first. Participants were timed on how long it took them to complete the course, as well as monitored by the test proctor for the number of collisions the participant had with obstacles while operating the simulated UAV. In addition, participants were asked to take a survey following completion of both types of the movement test, in which they remarked on which test they felt more comfortable with and which test felt closer to natural human vision. Both the quantitative data and qualitative survey responses were taken into account in the analysis of testing results.

The goal of the search and rescue test was to place the participant in a situation as close as possible to a real search and rescue scenario and analyze their performance while utilizing both stereoscopic and monoscopic version. This test was again conducted in both stereoscopic and monoscopic vision, and the order of each vision type was again randomized in a controlled fashion to ensure an equal number of participants began with either vision. In addition to two types of vision tests, there were two different search and rescue scenarios such that the participant flew one scenario first with one of the vision types, then flew the second scenario with the other vision type. The order of the scenarios was also randomized in a controlled manner. The scenario consisted of a forested and mountainous environment, a likely region for a search and rescue operation, which had figures placed at various points in the environment to represent victims. The participant operated the UAV while looking for the figures, or victims, hidden in the environment. If a figure was found, the participant had to identify some nearby characteristics of the environment, as well as the color of the dot on the figure's chest if they were able to visually identify it. The purpose of the colored dots was to quantify the participant's

ability to operate the UAV precisely enough to fly close to the victim, as well as the participant's ability to see detail with both vision types. Participants had ten minutes to fly around the environment and identify as many figures as possible. Participants were not told how many figures were present in the environment. The time at which they found each figure, the distinguishing features the participant identified near the figure, and the color of the dot on the figure's chest (if applicable) were all recorded. After this portion of the test, participants were asked to take another survey in which they identified which test felt more comfortable and which test felt closer to mimicking actual human vision. The full testing procedures, as well as the surveys utilized in the testing process, documents for IRB approval, and other testing-related documents, can be found in Appendix D.

IV. Results

A. Flight Simulation Results

In total, the team tested 18 participants in this study in an attempt to determine whether stereoscopic vision would improve the abilities of search and rescuers to navigate and identify individuals in an environment. All participants were University of Maryland, College Park students tested over the course of two weeks. The test plan is outlined in the testing methodology.

The first test conducted by all participants was the preliminary cylinder test. In the cylinder test, subjects attempted to line up two cylinders in both monoscopic and stereoscopic vision. The value at which the cylinder was off from the center was recorded. The subject attempted the test three times for both vision times. Figure 24 is the

average absolute value of the three measurements for each vision type. The units of the value are Unity units, the engine the test was created in. Unity units have no physical unit equivalent.

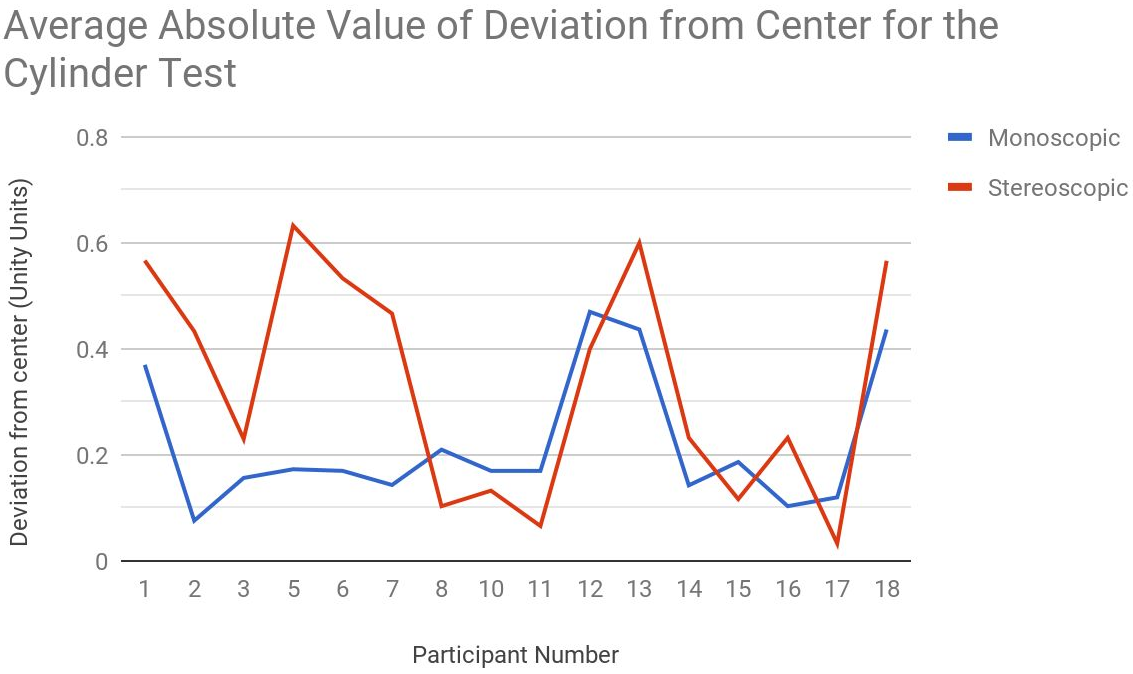

Figure 24: Graph of the average of the absolute value of each of the three measurements for each vision type. The complete version of this dataset can be viewed in Appendix E-2.

Overall, performance on the monoscopic version of the test was slightly better than performance on the stereoscopic test. This is also supported by the overall average value for the monoscopic test versus the stereoscopic test: 0.196 vs 0.296. However, in several cases individuals did significantly better on the stereoscopic version, sometimes achieving a value extremely close to 0. One factor that could have affected the cylinder test was that there was no limitation to the participants' field of view during the monoscopic version, so the participant could position their face at any position relative to

the screen without changing what was displayed on the screen itself, a feat not possible while wearing the Oculus. If the field of view for monoscopic vision was limited in a manner similar to the Oculus, then monoscopic vision may have less of an advantage.

In the next series of tests, the team assessed participants using a flight simulation in order to determine whether stereoscopic vision could improve UAV operations. Over the course of testing, it quickly became very clear that one of VR's main drawbacks was coming into play - nearly every one of the testing participants experienced VR sickness to some degree, suffering some sort of dizziness and nausea. Many participants noted that it was often due to the fact that, being inexperienced with the controls, they collided often with the ground or obstacles. This would cause the viewpoint to "clip" through the obstacle and cause various rapid visual artifacts, which would rapidly induce nausea and discomfort. However, even individuals who had a large amount of experience with flying UAVs or similar vehicles experienced discomfort while taking the test. It quickly became clear that VR sickness would be one of the greatest barriers to implementing this system as a regular feature of search and rescue operations.

Due to the proliferation of VR sickness, much of it due to camera viewpoint and control scheme issues in the flight simulation itself, the majority of the data gathered was inconsistent. Every participant completed the cylinder test; however, some participants started experiencing VR sickness when using the head mounted display during the flight simulation and therefore could not complete the rest of the movement test. Only approximately half of the subjects were able to reach the following search and rescue test,

with a much lower total completion rate. All conclusions extrapolated from the data were reached with this in mind.

A majority of the test subjects were inexperienced with UAV operation, with three having a moderate amount of experience and three having a great deal of experience amounting to over 300 hours of UAV flight time. All participants had little to no experience with virtual reality, an aspect that may have contributed to the high failure rates of the stereoscopic portions of the test.

Analyzing the results from the movement test became slightly more tricky. The movement test involved the user maneuvering a simulated UAV through a gradually more complex obstacle course. A quarter of the participants experienced discomfort upon taking the movement test and ended the test after a few minutes, resulting in very little useful data for those participants. However, a fairly significant number of participants managed to complete most or all of the movement test. Figure 25 compares the number of collisions with the environment that the participant had in both of the stereoscopic and monoscopic versions of the movement test for those that completed it.

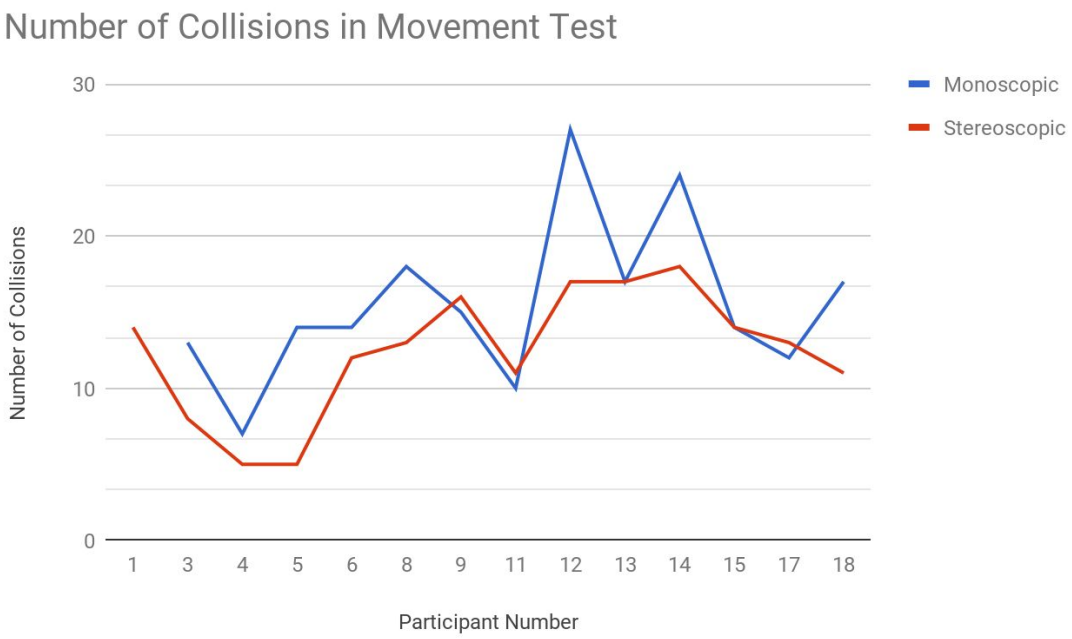

Figure 25: The number of collisions in the movement test for monoscopic vision versus stereoscopic vision. The complete dataset can be viewed in Appendix E-3.

The data demonstrates that, on average, participants collided with the environment slightly less in stereoscopic vision than in monoscopic vision. This demonstrates that stereoscopic vision assists the user with judging distances and obstacles slightly better than monoscopic vision does. The responses to the exit surveys also supported this fact, as a majority of participants answered that the stereoscopic vision test felt as though it more accurately mimicked human vision. Additionally, individuals tested who had experience operating UAVs with a first person viewpoint were more likely to complete the test and almost universally indicated that they preferred the operation of the stereoscopic test better, revealing that practice and comfort with the system increased favorability and usability of the system. Many beginners with no UAV experience also favored the stereoscopic test, showing that it was beginner-friendly and intuitive for some

individuals. Overall, on the movement test, both the number of collisions and the participant response to the test seemed to indicate that, while the stereoscopic test may not have been the more comfortable test to take, it felt more accurate and helpful to the user. This is an encouraging result and shows that a VR system would be well received by experienced operators.

	Q1: Overall, which test did you feel more comfortable with?	Q2: In your opinion, which test more accurately mimicked human vision?	Q3: Which test did you feel you did better on (e.g. completed course more quickly, ran into fewer obstacles)?	Q5: Overall, which test did you like better?
Monoscopic	6	4	4	4
Stereoscopic	7	8	9	7
Both Equally	1	2	1	3

Figure 26: Table displaying survey questions for the movement test along with number of responses of each answer type. Question 4 is not displayed because it simply asked whether or not the participant experienced VR sickness during the test. Full responses to the survey are available in Appendix E-5.

Despite almost universally experiencing discomfort in the stereoscopic test, participants indicated that they liked stereoscopic vision better for the purposes of maneuvering the UAV. Almost all of the negative comments indicated issues with the flight simulation - the viewpoint sometimes went through walls, the vehicle did not fly like a UAV, and so forth. A very common complaint was that the control scheme was very strange and hard to get used to, and several individuals commented that they felt like they did better on the second test simply because they had gotten more used to the controls. This issue could have been diminished by giving participants a longer period of time to acclimate in the tutorial. An individual who was very experienced with UAV

operation commented that the vehicle did not fly like a quadcopter. From other comments on the exit survey, this handling difference could stem from the control scheme, acceleration or flight path of the quadcopter, or numerous other issues. It is clear that a great source of inconsistency and difficulty in the test is the flight simulation itself, and if conducted again the study should use a different or more polished flight simulation with a better control scheme. Issues in particular that would need be resolved include the control scheme, which many participants identified as confusing, and several visual glitches that occurred when the UAV collided with a wall or the floor, which definitely contributed to discomfort among participants. If these issues could be resolved in the current flight sim that would certainly be advantageous for future testing, but if that is outside the capabilities of the current flight sim a different one may have to be used. Despite difficulty with the flight simulation, however, the data and survey results still supported stereoscopic vision as being a more favorable choice when maneuvering the UAV.

Even fewer participants were able to reach the search and rescue flight simulation portion of the test, and out of those individuals almost none managed to complete it. In this portion of the test, participants operated the simulation again, this time in a mountainous and forested terrain, in order to find figures scattered around the environment. This fact highlights, again, issues with the usability and comfort of the flight simulation, issues that would hopefully be dealt with in any future prototype of this system. Techniques to combat VR sickness are varied, and unfortunately were not able to be implemented in the flight simulation. The flight simulation was not optimized for the Oculus Rift, which needs 90 fps to reduce the chance of VR sickness. Due to the

complicated and layered simulation environment, particularly with this search and rescue test, the flight simulation became as low as 30 fps, which induced nausea to test participants. In the future, if the flight simulation frame rate is matched to that of the Oculus by simplifying the testing environment, the number of participants with VR sickness could be reduced. Figure 27 lists the outcomes of the participants who had any sort of significant results on the flight simulation test, including the number of figures they found and whether or not they finished the test.

Participant Number	Figures Found - Stereoscopic Vision	Figures Found - Monoscopic Vision	Finished Test
3	1	5	No
4	4	9	No
11	3	8	No
12	3	8	Yes
15	5	3	No
18	5	4	Yes

Figure 27: A selection of mostly complete or complete runs of the search and rescue test. Full results can be found in Appendix E-4.

Since so few individuals finished this portion of the test, it is difficult to ascribe any sort of quantitative analysis to this data. Individuals tended to find more figures in monoscopic vision, but only because most participants could not finish the stereoscopic test. Barring quantitative analysis, the team was able to look at the survey responses to the search and rescue portion to see if any conclusions can be drawn from this part of the test.

	Q1: Overall, which test did you feel more comfortable with?	Q2: In your opinion, which test more accurately mimicked human vision?	Q3: Which test did you feel you did better on (e.g. completed course more quickly, ran into fewer obstacles)?	Q5: Overall, which test did you like better?
Monoscopic	5	1	5	4
Stereoscopic	1	6	2	2
Both	1	0	0	1

Figure 28: Table displaying survey questions for the search and rescue test along with number of responses of each answer type. Question 4 is not displayed because it simply asked whether or not the participant experienced VR sickness during the test. Full responses to the survey are available in Appendix E-6.

Survey responses for the search and rescue test leaned far more towards favoring monoscopic vision. This can mostly likely be attributed, however, to the flight simulation once again, as a majority of the individuals did not complete the stereoscopic portion of the test due to VR sickness. A much higher level of discomfort was experienced overall by participants during the stereoscopic version of the test, so it is only logical that they would indicate that they felt more comfortable with the monoscopic test. However, most participants still indicated that the stereoscopic test still felt more accurate to human vision. One participant explicitly commented on their exit survey that they would have favored the stereoscopic vision version if it did not make them sick, indicating that the main drawback was not the stereoscopic vision itself but its side effects which could be mitigated through several unincorporated techniques. The longer duration of the search and rescue test was the greatest difference between the movement test and the search and rescue test and contributed greatly to the increased level of discomfort experienced by participants. Several participants also commented that the monoscopic version of the test

did not allow them to alter the viewpoint of the UAV, which made searching for and identifying figures more difficult. Based on the results for the movement test, if the stereoscopic search and rescue test was more comfortable to operate, operators would likely be more inclined to favor stereoscopic over monoscopic vision.

In summary, it is hard to come to any solid conclusions based on the result of these tests. The flight simulation was the source of a lot of inconsistencies and had a large effect on this study's testing base. It is hard to say conclusively and quantitatively that stereoscopic vision is better than monoscopic vision; however, many participants vocally favored stereoscopic vision, even in situations where they experienced discomfort as a result of the flight simulation's lack of optimization for virtual reality usage. This result still supports the team's goal, as part of the aim of this system is to create an intuitive prototype that supports the abilities of the operator. With a refined flight sim and control scheme, the benefits of stereoscopic vision would not only increase but the system would also be more comfortable and intuitive for the user. If this test were to be conducted again the future, a flight simulation better optimized for virtual reality and with a control scheme more similar to how UAVs operate in actuality would both be musts. The results show that users do prefer stereoscopic vision over monoscopic vision on a qualitative level, and that the main roadblocks to overcome are ease of usage and comfort, so users are able to utilize a VR system for extended periods of time while searching for victims.

B. Full System Results and Specifications

A fully functional gimbal was created to match the mission requirements, as assembled in the following figure:

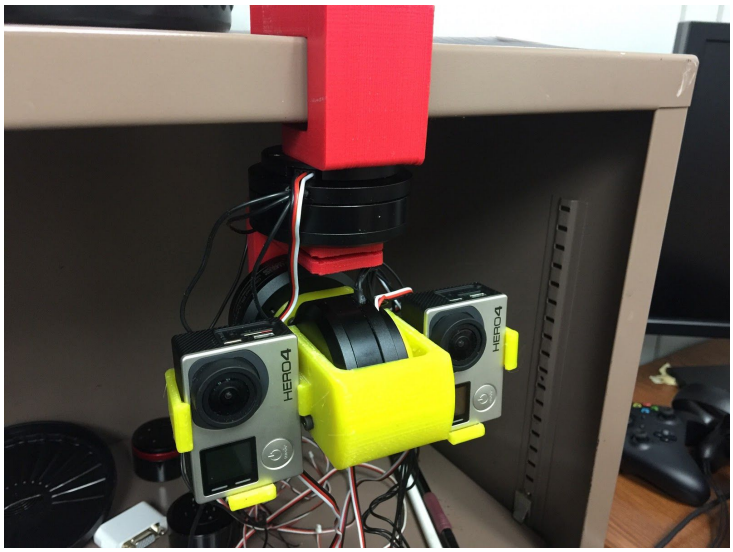

Figure 29: Final assembled gimbal.

The payload component can be easily attached and detached from a commercial UAV, due to its small size and weight. The gimbal is 218mm high, 141mm wide, and 123mm deep, and weighs 985 grams, including the two GoPro HERO4 Black cameras attached. In addition, the gimbal is powered by two standard 11.1V LiPo battery packs, that can be easily mounted onto the UAV. The gimbal successfully rotates in the axes necessary to match a user's head movements. The yaw axis controlled rotation ranges from 139° to 340°, while the pitch axis controlled rotation ranges from 36° to -32°, as showcased in Figure 30 and Figure 31 respectively.

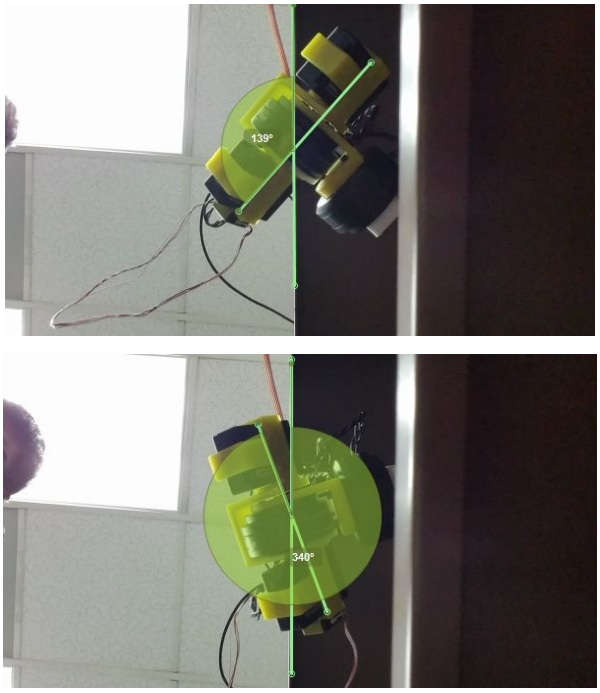

Figure 30: Yaw axis control of custom gimbal at 139° (top) / 340° (bottom).

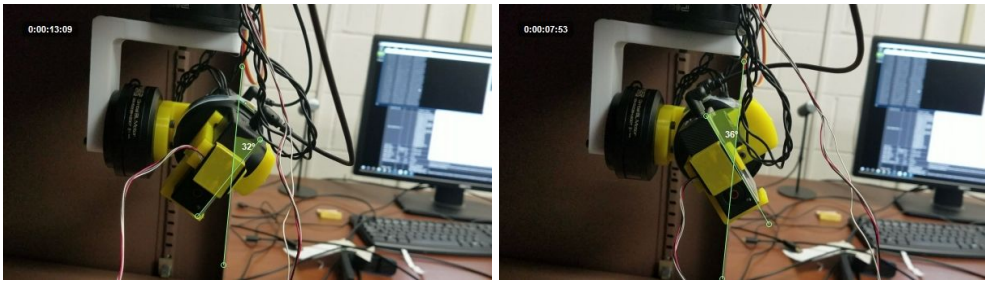

Figure 31: Pitch axis control of custom gimbal at 36° (left) / -32° (right).

At the maximum controlled rotation speed of 13.3 degrees per second, it can easily synchronize with the user. From the results of the initial communications range test, the gimbal will be able to receive user commands from a distance of 425.4 ft in an crowded, urban environment when paired with the Connex transmission equipment. The video transmission rate remains at 120 frames per second with 1080p resolution.

V. Conclusion

UAVs used in tandem with VR and AR technology offer unique advantages in managing SAR operations. UAVs allow for a more efficient and rapid search while keeping the operator out of harm's way, and VR and AR technology allows for an operator to have a more realistic and in-depth view of the environment in order to easily find points of interest. Merging these technologies creates a complex system that allows for a more detailed overhead visual search of search and rescue areas while operating a comfortable and intuitive VR and AR interface.

In this paper, the team reviewed the literature regarding the costs and benefits of various UAV models, various user interfaces, and modern VR technologies. Additionally, ARM IT explored alternative methods of interacting with a UAV. Several methods exist for controlling a UAV, ranging from a physical control to a graphical interface. Additionally, numerous options exist for communicating with the UAV at a distance, often with a trade-off of improved reception for more power consumption. The preferred method of controlling a UAV is through a combination of stereoscopic camera inputs linked to the HMD and an AR interface overlaid onto the video feed. Through an intelligent combination of these features, the efficiency and ease of using UAVs in search and rescue situations can be improved.

The team also discussed the methodology used to construct the prototype system. The hardware of this project consisted of a custom built gimbal system, which was constructed to hold two GoPro cameras. The gimbal communicates with head movement data from the Oculus Rift in order to correspond with the head movements of the user. In

turn, the two cameras send a stereoscopic video feed to the user, which is viewed through the Oculus Rift. Additionally, the team constructed basic overlays for the virtual reality feed as a starting point for future prototypes to create more complex overlays that communicate important data to the user in real time. Furthermore, Team ARM IT sought to support their hypothesis through a flight simulation test, in which participants conducted a movement and search-and-rescue test in both monoscopic and stereoscopic vision in order to show that stereoscopic vision improved the quality of searching and allowed users to judge their surroundings more accurately. While the results of this survey were far from conclusive, the survey results showed to some degree that users felt the stereoscopic vision system was more like human vision and assisted them in both the movement and search-and rescue-aspects of the study.

In the end, the team's working prototype showed that it was possible to stream live stereoscopic video feeds from twin cameras to an Oculus Rift, and in turn the Oculus Rift could dictate the movement of the gimbal to match the user's head movements. The prototype also showed that an overlay system was possible, leaving that as a task for future research. Finally, the team's research showed that users would prefer a stereoscopic system for the purposes of search and rescue in the future.

The results of this research could greatly impact how SAR operations are conducted. The VR/AR interface can increase SAR success rates by decreasing the cost in human resources and search time while reducing injuries to both searchers and victims, as well as providing a real-time stereoscopic vision feed and overlays of real-time information to the operator. In the future, a system based on this prototype could be used

in high-risk SAR operations to find lost individuals quickly and safely in dangerous, rapidly changing environments.

Appendix

Appendix A: Computer Parts List

Original PC Parts List

CPU	Intel - Core i7-4770 3.4GHz Quad-Core Processor
Motherboard	MSI - Z97-GAMING 5 ATX LGA1150 Motherboard
RAM	Corsair - Vengeance Pro 16GB (2 x 8GB) DDR3-1866 Memory
Storage	Western Digital - Caviar Blue 1TB 3.5" 7200RPM Internal Hard Drive, Kingston - SSDNow V300 Series 120GB 2.5" Solid State Drive
Video Card	EVGA - GeForce GTX 980 Ti 6GB Superclocked+ ACX 2.0+ Video Card
Case	Corsair - 200R ATX Mid Tower Case
PSU	EVGA - SuperNOVA G2 750W 80+ Gold Certified Fully-Modular ATX Power Supply

Testing Station PC Parts List

CPU	AMD - Threadripper 1950X 3.4GHz 16-Core Processor
CPU Cooler	Enermax LIQTECH TR4 360mm AIO Liquid CPU Cooler
Motherboard	Asus - ROG ZENITH EXTREME EATX TR4 Motherboard
RAM	32GB Corsair Vengeance LPX 3200MHz
Storage	SAMSUNG 960 EVO M.2 500GB NVMe PCI-Express 3.0 x4 Internal Solid State Drive
Video Card	AMD - Vega Frontier Edition 16GB

	Frontier Edition Video Card
Case	Corsair Obsidian Series 750D Full-Tower
PSU	EVGA - SuperNOVA P2 1200W 80+ Platinum Certified Fully-Modular ATX Power Supply

Appendix B: Code Debugging Errors

LNK1104: LibOVR could not be opened	Change Oculus libraries to current version of Visual Studio
LNK2038: mismatch detected	Change the Runtime Library in the project properties page (under code generation) to /MT or static linking
LNK2019: Unresolved external signals LNK1120: unresolved errors	Use the exact name of the libraries to be included with the linking process (including the library names itself). For example: Adding *opencv_world310.lib* to Linker->Input->Additional Dependencies
SDL2 is missing: error pop-up	Copy *SDL2.dll* into the build folder of the project
LNK1104: could not open opencv_world310.lib	Add a line *D:\ZED_SDK\dependencies\opencv_3.1.0\x64\vc14\lib* in Properties->VC++ Directories-> Library Directories
LNK2038: mismatch detected for _ITERATOR_DEBUG_LEVEL: value 0 does not match value 2 in Shader.obj	Set *_ITERATOR_DEBUG_LEVEL* to the appropriate value in all projects and sources
LNK1181: cannot open opencv_world.lib	Project->Properties->VC++ Directories->Library Directories->Add path for opencv library
Cmake errors	Copying *SDL2 dll*, *opencv_world310.dll*, and *glew dll* into the build directory

Appendix C: Code

The code for the Camera to Oculus Translation (C++) and the Head Tracking Code (Python) can be found through this link: https://github.com/TeamArmIt

Appendix D: Testing Documents

Appendix D-1: Testing Procedure Revision # 0.13

TEAM ARM-IT

STEREOSCOPIC TESTING PROCEDURE

GLOSSARY

CPU – Central Processing Unit

GPU – Graphics Processing Unit

HMD – Head mounted display

Oculus – Oculus Rift (a brand specific HMD)

SAR – Search and Rescue

US – United States

MATERIALS

To ensure a fair testing environment, similar if not identical hardware is to be utilized. To this end two high end computers will be used to run the simulations. The computers will consist of a 1950X Ryzen™ Threadripper™ CPU and a Radeon™ Vega Frontier Edition GPU. This will ensure that the hardware does not cause any input lag or drop frames which could affect the test participant.

The head mounted display (HMD) to be used will be an Oculus Rift.

A third computer shall be utilized as a central repository of participant data to ensure no participant performs the testing procedure more than once.

PARTICIPANT SELECTION

Participants are to be selected based on their willingness to test experimental software and explore virtual reality. They are to be able to use virtual reality without nausea or discomfort.

TEST INITIALIZATION

The test proctor will verify that the participant has not previously participated by cross-referencing the participant's name and email address on the central computer. The participant will then be assigned a unique identification number which will be recorded on all worksheets to be used during the testing procedure.

The test proctor will obtain a testing kit which will contain the following materials:

- One (1) Blue ballpoint pen
- One (1) Clipboard

- One (1) Worksheet A
- One (1) Worksheet B

After collecting the testing kit, the proctor will escort the participant to the testing station and record which station is being used on Worksheet A. Participants are to be seated at one of the two testing stations. A test proctor will remain in the room with the participant. The participant will place the Oculus on their head and will make adjustments to ensure that the fit is proper and comfortable.

TESTING PROCEDURE

CYLINDER TEST

The test proctor will load up the cylinder test. The participant will take the cylinder test and the proctor will record the result. The participant must attempt to line up the two elements in the cylinder test while viewing it with stereoscopic vision. The participant will attempt this test three times.

MOVEMENT TEST

The test proctor will ask the participant to pick a slip of paper out of a hat and record the result in Worksheet A. The slip will denote whether the monoscopic or stereoscopic version of the test will be done first. The test proctor will load up the appropriate test according to this result.

The test proctor will record the time to complete the course in addition to the number of collisions with the surroundings the participant makes on the form from Appendix A.

After the participant has completed one version of the Movement Test, the proctor will load the other version for the participant to complete, recording the same data as before.

This concludes the Movement test.

SEARCH AND RESCUE TEST

The proctor will have the participant pick out of a hat. The result will denote which variant of the search and rescue test will be done first and whether it will be done in monoscopic or stereoscopic version.

Note: File structure – SAR_1_B denotes Search and Rescue test, Scenario 1, Variant B.

The appropriate file will be loaded, and the participant will be instructed to find as many of the 15 humanoid figures as they can within five minutes. The participant must notify the proctor when they believe they have located a figure and provide any additional details about the figure that they can. Instruct the participant to estimate the location of the figure in relation to its surroundings.

Example: Participant believes to have located a figure between two trees, the participant will declare which tree the figure is closest to and provide the color of the circle and numeric character on the figure's chest.

The proctor will start a five-minute timer. The proctor will record when (time in minutes and seconds) the participant believes to have located a figure (in column two of Worksheet B) and the additional information the participant provides.

At the end of five minutes or when the participant has located all 15 figures, whichever comes first, the proctor will instruct the participant to cease any movements with regards to the simulation. The proctor will then load the unused variant for that scenario.

Example: If the first SAR test was Scenario 2, monoscopic; the proctor should load Scenario 2, stereoscopic. i.e. SAR_2_A used first, then SAR_2_B for the second test.

The proctor will conduct the second test in the same manner as the first, recording the same types of data as before.

Upon completion of the second SAR test, the proctor will instruct the participant to remove the HMD. The proctor will thank the participant for their assistance in this test. The proctor will offer the survey to the participant and will escort the participant from the laboratory.

POST TEST

The proctor will close all programs related to testing and return the testing kit to the central station.

Appendix D-2: Test Proctor Checklist

PROCTOR CHECKLIST

1. Give participant both (2) copies of consent form and read script. The participant must sign both.
2. Prepare WORKSHEET A and WORKSHEET B labelled with participant number. Worksheets are located in primary test room on shelf. Retrieve participant information sheet from top drawer of storage cabinet labelled Switches in back of lab. Add participant information to the participant information sheet. The email must be the student's umd email.
3. Escort participant to available testing station. Record which station is being used on WORKSHEET A.
4. Have participant pick one piece out of hat 1 for WORKSHEET A. **DO NOT PUT THE PAPER BACK IN THE HAT!!!!!!!!!**
5. Place Oculus on participant's head. Ensure fit is comfortable and participant is satisfied before continuing. Can use switch on bottom to adjust. *Note: Glasses should be removed prior to putting Oculus on participants head. Remove Oculus and continue to next step.
6. On Desktop, right click the background and select AMD Radeon Pro and AMD FirePro Settings. Hit the ReLive, ensure ReLive is on and Record Desktop is enabled. Press ctrl-shift-R to start the recording and verify recording has started where a timer should appear. Minimize the AMD window (DO NOT CLOSE).
7. Load up CYLINDER TEST. For steps a and b start with the letter that was picked out of the hat and then run the opposite test.

a. For monoscopic: Open Testing Folder Unity version 5.3.1f1 and select Unity Test from recently opened files. Select game tab on the top of the lower panel and ensure "Maximize on Play" is selected as a lighter gray than the other buttons. Press play. Participant can use up and down arrow keys to align cylinders. After aligning, hold down enter to show number. Record number to 3 decimal places on worksheet A. Hit pause after you record the measurement to end the trial. Hit play one time to reset the cylinders to their original positions and then hit play again to restart the test for another trial. Allow participant to complete CYLINDER TEST three times and record results on worksheet A.

b. For stereoscopic: Participant must have Oculus on head before file is opened. Open the Stereoscopic_Test.exe file and press play. Press down for a bit to reset test. For the stereoscopic test, the participant must have the Oculus on their head in order to get the distance/ move the cylinders. Participant can use up and down arrow keys, and press enter to show number. Record number on worksheet A. Alt-Tab out of the Test, and right click "Close". Reopen the file to begin a new

trial. Allow participant to complete CYLINDER TEST three times and record results on worksheet A. Remove Oculus.

8. Load up TUTORIAL on computer (Landscape Map) (Folder*: 2_SARTest, which is the SARTest Unreal Engine Project File with the blue circle icon,* In FIle*: bottom left corner, click content->maps , double click Landscape Map*). Double click Landscape Map in Maps folder under Content. Press the drop down button to the right of the play button. If the participant has selected A, they will start with monoscopic. To run the monoscopic test, press Selected Viewport. If the participant has selected B, ensure the participant has the Oculus on and press VR Preview. Press F to change into first person view. Press F11 for full-screen. Give participants 2-3 minutes with the tutorial. To move around, the left joystick controls altitude and speed, right stick controls direction. Participants can end tutorial after 2 minutes if they so desire, but proctor must move on with test after 3 minutes. Press escape to exit the test. **This procedure is to be performed only once per participant.**
9. Return to Testing folder on desktop.
10. Load up MOVEMENT TEST on computer based on result of step 4. (*double click on 1_MovementTest-> MyProject with the blue circle icon*). Using the drop down arrow next to play, select Selected Viewport for monoscopic, and VR Preview for stereo. Press F to change into First Person View.
11. Verbally instruct participant to follow the blue rings without flying over the walls until you reach the dark shiny cone or run out of time. Observe participant and count number of collisions using tally marks on WORKSHEET A. Record number of collisions and completion time. Have participant begin test and start the timer. The participant has 10 minutes to complete this test.
12. Repeat steps 10 and 11 for untested vision mode.
13. Give participant SURVEY 1 for the MOVEMENT TEST. Record on survey that it is for the MOVEMENT TEST.
14. Have participant pick out of hat 2 for SEARCH AND RESCUE TEST. **DO NOT PUT THE PAPER BACK IN THE HAT!!!!!!!!!**
15. Load up SEARCH AND RESCUE TEST on computer. (*Desktop->test folder-> 2_SARTest->double click blue circle ico*n)
16. Click content in bottom left corner-> maps-> double click SAR_1 or SAR_2 based on the letter picked (W,X,Y,Z). Using the down arrow next to play, select Selected Viewport for monoscopic, and VR Preview for stereo. Press F to change into First Person View.
17. Verbally instruct participant: “you will now complete a simulated search and rescue task to find the lost humanoid figures. In order to find a figure, you must identify when you see the figure, if you can navigate close to the figure, please

tell me the color of the colored circle on the chest, and the closest object to the figure."

18. Have participant begin test and start 10 minute timer. Record the countdown timer time when the participant believes they have found a target and any details given verbally about the target on Worksheet B.
19. If participant finds all 15 figures, stop the test and record the time. Stop the test once the timer run out.
20. Repeat steps 16-19 with the other SAR Map and other vision setting.
21. Tell participant this portion of the test is over. Place Oculus on table by monitor.
22. Close program and press CTRL-Shift-R to stop the recording.
23. Give participant SURVEY 2 for the SEARCH AND RESCUE TEST. Record on survey that it is for the SEARCH AND RESCUE TEST.
24. Give the participant the participant copy of the consent form and thank for participation. Remind them that we will hold a raffle at the conclusion of testing period for the gift card and will contact the winner.
25. Escort participant from lab.
26. Go back to computer->desktop-> Test folder-> test recordings and rename the recording file to <participant #>_date like the sample in the folder.
27. Place worksheets and surveys in top drawer of storage cabinet labelled Switches in back of lab underneath the participant list.
28. Reset test station and return other equipment to appropriate places.

**For monoscopic vision - selected viewpoint

**For stereoscopic vision - VR preview

Appendix D-3: Procedure Consent Form

TEAM ARM IT
Consent Form

Project Title	*Augmented and Virtual Reality in Relation to UAV Capabilities*
Purpose of the Study	*This research is being conducted by **Dr. Anil Deane** at the University of Maryland, College Park. The purpose of this research project is to test mono and stereoscopic vision using virtual reality.*
Procedures	*The procedures involve interacting with a virtual environment to search for objects, once while wearing the Oculus Rift and once while not wearing the Rift. You will also operate a flight simulation once while wearing the Oculus Rift and once while not wearing the Rift. You will fill out a questionnaire about your experience following both tests.*
Potential Risks and Discomforts	*There may be some risks from participating in this research study. Some dizziness and motion sickness may result from wearing and operating the Oculus Rift. You may end your participation in the study at any time if you find yourself experiencing discomfort. Any record of your participation, as well as any premature results, will be removed from the study data.*
Potential Benefits	*There are no direct benefits from participating in this research. However, possible benefits include the opportunity to try the Oculus Rift and operate a flight simulation. We hope that, in the future, other people might benefit from this study through improved understanding of virtual reality and stereoscopic vision and how it could be used to improve UAV operations.*
Confidentiality	*Any potential loss of confidentiality will be minimized by storing any personal information on a secure computer. Very little/no personal information will be collected.* *If we write a report or article about this research project, your identity will be protected to the maximum extent possible. Your information may be shared with representatives of the University of Maryland, College Park or governmental authorities if you or someone else is in danger or if we are required to do so by law.*

Medical Treatment [*If Necessary]	*The University of Maryland does not provide any medical, hospitalization or other insurance for participants in this research study, nor will the University of Maryland provide any medical treatment or compensation for any injury sustained as a result of participation in this research study, except as required by law.*
Compensation [*If Necessary]	*If you wished to be entered into the $10 gift card raffle, only your name and email address will be collected to receive compensation.*
Right to Withdraw and Questions	*Your participation in this research is completely voluntary. You may choose not to take part at all. If you decide to participate in this research, you may stop participating at any time. If you decide not to participate in this study or if you stop participating at any time, you will not be penalized or lose any benefits to which you otherwise qualify.* *If you decide to stop taking part in the study, if you have questions, concerns, or complaints, or if you need to report an injury related to the research, please contact the investigator:* ***Dr. Anil Deane*** ***301 - 406 - 4866*** ***deane@umd.edu***
Participant Rights	*If you have questions about your rights as a research participant or wish to report a research-related injury, please contact:* **University of Maryland College Park** **Institutional Review Board Office** **1204 Marie Mount Hall** **College Park, Maryland, 20742** **E-mail: irb@umd.edu** **Telephone: 301-405-0678** *This research has been reviewed according to the University of Maryland, College Park IRB procedures for research involving human subjects.*
Statement of Consent	*Your signature indicates that you are at least 18 years of age; you have read this consent form or have had it read to you; your questions have been answered to your satisfaction and you voluntarily agree to participate in this research study. You will receive a copy of this signed consent form.* *If you agree to participate, please sign your name below.*

Signature and Date	**NAME OF PARTICIPANT [Please Print]**	
	SIGNATURE OF PARTICIPANT	
	DATE	

Appendix D-4: Worksheet A

WORKSHEET A

Proctor: _____ **Test Station**: _____ **Participant ID #**: _____

Test Date: Month_____ Day _____ 2018

Hat Result (Circle One): **A (Monoscopic first)** **B (Stereoscopic first)**

Cylinder Test

Mono Cylinder	Distance	Stereo Cylinder	Distance
1		1	
2		2	
3		3	

Movement Test

First Run

Circle one: **Mono Stereo**

Time to Complete: Minutes _____ Seconds _____

Number of Collisions: _____

Notes:

Second Run

Circle one: **Mono Stereo**

Time to Complete: Minutes _____ Seconds _____

Number of Collisions: _____

Notes:

Appendix D-5: Worksheet B

WORKSHEET B

Proctor: _____ **Test Station**: _____ **Participant ID #**: _____

Hat Result (circle one):

W (monoscopic first, SAR_1 first) **X** (monoscopic first, SAR_2 first)

Y (stereoscopic first, SAR_1 first) **Z** (stereoscopic first, SAR_ 2 first)

First Run

Scenario: **1 2** Vision: **Mono Stereo**

Figure Found	**Time Found**	**Color**	**Figure Number**	**Object**
1				
2				
3				
4				
5				
6				
7				
8				
9				
10				
11				
12				
13				
14				
15				

Second Run

Scenario: **1 2** Vision: **Mono Stereo**

Figure Found	Time Found	Color	Figure Number	Object
1				
2				
3				
4				
5				
6				
7				
8				
9				
10				
11				
12				
13				
14				
15				

Notes:

The first column in the table is to record the order in which the figures are found, **not the figure number itself.**

Appendix D-6: Post-Movement Test Survey

TEAM ARM IT: *Augmented and Virtual Reality in Relation to UAV Capabilities*
This survey should be administered after the participant has taken both test 1 and test 2 of the MOVEMENT test. Test 1 refers to the test you took first chronologically. Test 2 refers to the test you took second chronologically.

Please answer all questions based on your experience with the MOVEMENT test *only*.

1. Overall, which test did you feel more comfortable with?

Test 1 Test 2 Both were equally comfortable

2. In your opinion, which test more accurately mimicked human vision?

Test 1 Test 2 Both felt equally accurate

3. Which test did you feel you did better on (e.g. found more objects, completed in a shorter amount of time)?

Test 1 Test 2 I felt I did equally well on both

4. Did you experience any motion/virtual reality sickness while operating either test?

Yes No

If yes, how severe was your motion sickness or discomfort? Did you feel it seriously inhibited your ability to take the test?

_____

_____

_____

_____

5. Overall, which test did you like better? (Pick test 1, test 2, equally comfortable with both)

Test 1 Test 2 I liked both equally

6. Do you have any other comments?

_____

_____

_____

_____

Appendix D-7: Post Flight Simulation Survey

TEAM ARM IT: *Augmented and Virtual Reality in Relation to UAV Capabilities*
This survey should be administered after the participant has taken both test 1 and test 2 of the SEARCH AND RESCUE test. Test 1 refers to the test you took first chronologically. Test 2 refers to the test you took second chronologically.

Please answer all questions based on your experience with the SEARCH AND RESCUE test *only*.

1. Overall, which test did you feel more comfortable with?

Test 1 Test 2 Both were equally comfortable

2. In your opinion, which test more accurately mimicked human vision?

Test 1 Test 2 Both felt equally accurate

3. Which test did you feel you did better on (e.g. completed course more quickly, ran into fewer obstacles)?

Test 1 Test 2 I felt I did equally well on both

4. Did you experience any motion/virtual reality sickness while operating either test?

Yes No

If yes, how severe was your motion sickness or discomfort? Did you feel it seriously inhibited your ability to take the test?

_____

_____

_____

_____

5. Overall, which test did you like better? (Pick test 1, test 2, equally comfortable with both)

Test 1 Test 2 I liked both equally

6. Do you have any other comments?

_____

_____

_____

_____

Appendix D-8: IRB Approval Document (Initial)

UNIVERSITY OF MARYLAND
INSTITUTIONAL REVIEW BOARD

1204 Marie Mount Hall
College Park, MD 20742-5125
TEL 301.405.4212
FAX 301.314.1475
irb@umd.edu
www.umresearch.umd.edu/IRB

DATE:	March 8, 2017
TO:	Anil Deane
FROM:	University of Maryland College Park (UMCP) IRB
PROJECT TITLE:	[1021303-1] Team ARM IT
REFERENCE #:	
SUBMISSION TYPE:	New Project
ACTION:	APPROVED
APPROVAL DATE:	March 8, 2017
EXPIRATION DATE:	March 7, 2018
REVIEW TYPE:	Expedited Review
REVIEW CATEGORY:	Expedited review category # 7

Thank you for your submission of New Project materials for this project. The University of Maryland College Park (UMCP) IRB has APPROVED your submission. This approval is based on an appropriate risk/benefit ratio and a project design wherein the risks have been minimized. All research must be conducted in accordance with this approved submission.

Prior to submission to the IRB Office, this project received scientific review from the departmental IRB Liaison.

This submission has received Expedited Review based on the applicable federal regulations.

This project has been determined to be a Minimal Risk project. Based on the risks, this project requires continuing review by this committee on an annual basis. Please use the appropriate forms for this procedure. Your documentation for continuing review must be received with sufficient time for review and continued approval before the expiration date of March 7, 2018.

Please remember that informed consent is a process beginning with a description of the project and insurance of participant understanding followed by a signed consent form. Informed consent must continue throughout the project via a dialogue between the researcher and research participant. Unless a consent waiver or alteration has been approved, Federal regulations require that each participant receives a copy of the consent document.

Please note that any revision to previously approved materials must be approved by this committee prior to initiation. Please use the appropriate revision forms for this procedure.

All UNANTICIPATED PROBLEMS involving risks to subjects or others (UPIRSOs) and SERIOUS and UNEXPECTED adverse events must be reported promptly to this office. Please use the appropriate reporting forms for this procedure. All FDA and sponsor reporting requirements should also be followed.

All NON-COMPLIANCE issues or COMPLAINTS regarding this project must be reported promptly to this office.

Please note that all research records must be retained for a minimum of seven years after the completion of the project.

If you have any questions, please contact the IRB Office at 301-405-4212 or irb@umd.edu. Please include your project title and reference number in all correspondence with this committee.

This letter has been electronically signed in accordance with all applicable regulations, and a copy is retained within University of Maryland College Park (UMCP) IRB's records.

Appendix D-9: IRB Approval Document (Extension)

UNIVERSITY OF MARYLAND
INSTITUTIONAL REVIEW BOARD

1204 Marie Mount Hall
College Park, MD 20742-5125
TEL 301.405.4212
FAX 301.314.1475
irb@umd.edu
www.umresearch.umd.edu/IRB

DATE:	March 4, 2018
TO:	Anil Deane
FROM:	University of Maryland College Park (UMCP) IRB
PROJECT TITLE:	[1021303-2] Team ARM IT
REFERENCE #:	
SUBMISSION TYPE:	Continuing Review/Progress Report
ACTION:	APPROVED
APPROVAL DATE:	March 4, 2018
EXPIRATION DATE:	March 7, 2019
REVIEW TYPE:	Expedited Review
REVIEW CATEGORY:	Expedited review category # *8 (b)*

Thank you for your submission of Continuing Review/Progress Report materials for this project. The University of Maryland College Park (UMCP) IRB has APPROVED your submission. This approval is based on an appropriate risk/benefit ratio and a project design wherein the risks have been minimized. All research must be conducted in accordance with this approved submission.

Prior to submission to the IRB Office, this project received scientific review from the departmental IRB Liaison.

This submission has received Expedited Review based on the applicable federal regulations.

This project has been determined to be a Minimal Risk project. Based on the risks, this project requires continuing review by this committee on an annual basis. Please use the appropriate forms for this procedure. Your documentation for continuing review must be received with sufficient time for review and continued approval before the expiration date of March 7, 2019.

Please remember that informed consent is a process beginning with a description of the project and insurance of participant understanding followed by a signed consent form. Informed consent must continue throughout the project via a dialogue between the researcher and research participant. Unless a consent waiver or alteration has been approved, Federal regulations require that each participant receives a copy of the consent document.

Please note that any revision to previously approved materials must be approved by this committee prior to initiation. Please use the appropriate revision forms for this procedure.

All UNANTICIPATED PROBLEMS involving risks to subjects or others (UPIRSOs) and SERIOUS and UNEXPECTED adverse events must be reported promptly to this office. Please use the appropriate reporting forms for this procedure. All FDA and sponsor reporting requirements should also be followed.

All NON-COMPLIANCE issues or COMPLAINTS regarding this project must be reported promptly to this office.

Please note that all research records must be retained for a minimum of seven years after the completion of the project.

If you have any questions, please contact the IRB Office at 301-405-4212 or irb@umd.edu. Please include your project title and reference number in all correspondence with this committee.

This letter has been electronically signed in accordance with all applicable regulations, and a copy is retained within University of Maryland College Park (UMCP) IRB's records.

Appendix E: Testing Data

Appendix E-1: Participant Information

Participant	UAV Experience Level	Completed? Y/N	VR Exp (hrs)
1	0	N	0
2	0	Y*	0
3	2	Y*	0
4	300	Y	0
5	0	N	3
6	0	N	0
7	0	N	0
8	0	N	0
9	0	N	0
10	40	N	0
11	300	N	Did not denote
12	300	Y*	0
13	0	N	0
14	2	N	1.5
15	0	N	0
16	0	N	0
17	20	N	0
18	0	Y	0

*Participant began at least one test but did not complete it

Appendix E-2: Cylinder Test Data

Participant	Mono Cylinder 1	Mono Cylinder 2	Mono Cylinder 3	Stereo Cylinder 1	Stereo Cylinder 2	Stereo Cylinder 3
1	0.77	0.17	0.17	0.7	0.4	0.6
2	0.029	-0.17	0.029	-0.4	-0.4	-0.5
3	0.0299	-0.07	-0.37	-0.5	-0.1	0.09
4	7.4	7.6	7.7	-0.4	-0.5	-0.1
5	-0.37	0.029	0.12	0.199	0.599	1.1
6	-0.27	-0.07	-0.17	0.3	0.6	0.7
7	0.13	0.23	-0.07	0.4	0.3	0.7
8	0.33	0.23	0.07	0	0.01	0.3
9	8.199	7.299	7.799	0.3999	0.099	0.599
10	-0.07	-0.27	-0.17	-0.2	0.099	0.099
11	-0.17	-0.17	-0.17	0.099	-4.17E-07	0.099
12	-0.17	-0.37	-0.87	-0.6	-0.3	-0.3
13	-0.57	-0.47	-0.27	-0.2	-0.6	-1
14	-0.07	0.229	0.129	0.199	0.299	0.199
15	-0.37	-0.17	0.02	0.05	0	-0.3
16	-0.17	-0.07	-0.07	0.399	-0.099	-0.199
17	0.02	-0.07	0.27	-0.099	0	0
18	-0.27	-0.57	-0.47	-0.8	-0.3	0.599

Appendix E-3: Movement Test Data

Participant	First Run Type	First Run Collisions	First Run Time	Second Run Type	Second Run Collisions	Second Run Time
1	Stereo	14	Incomplete	N/A	N/A	N/A
2	Stereo	6	Stopped at 1:35	Mono	9	4:47
3	Mono	13	2:59	Stereo	8	Quit at 1:56
4	Stereo	5	1:53	Mono	7	1:40
5	Stereo	5	Incomplete	Mono	14	3:45
6	Stereo	12	3:46	Mono	14	3:20
7	Stereo	10	Incomplete	N/A	N/A	N/A
8	Mono	18	1:39	Stereo	13	1:26
9	Mono	15	3:36	Stereo	16	1:51
10	Stereo	4	Stopped at 1:30	N/A	N/A	N/A
11	Mono	10	3:31	Stereo	11	2:34
12	Mono	27	3:48	Stereo	17	2:51
13	Mono	17	3:08	Stereo	17	2:03
14	Stereo	18	Stopped at 4:41	Mono	24	3:54
15	Stereo	14	1:38	Mono	14	1:29
16	Stereo	5				
17	Mono	12	2:50 - skipped last 3 corridors by flying over walls	Stereo	13	2:26
18	Mono	17	2:53	Stereo	11	2:43 - flew off course for 30 s

Appendix E-4: Search and Rescue Test Data

Participant	First Run Scenario	First Run Vision	Figures Found (list time, color, number, object)	Second Run Scenario	Second Run Vision	Figures Found
1	1	Stereo	1, 0:34, Red, Bridge	2	Mono	N/A
2	N/A	N/A	N/A	N/A	N/A	N/A
3	SAR 2	Mono	1, 0:34, Yellow, Tree; 2, 0:45, Pink, Tree; 3, 2:47, Blue, Rock; 4, 4:17, Green, Tree; 5, 6:49, Light blue, lake	SAR 1	Stereo	1, 1:23, Pink, Tree; Quit at 3:02
4	SAR 1	Mono	1,1:03, green, 2, 3:00, blue, 3 4:00, red, 4, 5:00, red, 5, 7:10, green, 6, 7:40, blue, 7, 8:20, red, 8, 9:00, brown, 9, 9:59, no color	2	Stereo	1,1:25, pink, 2, 3:10, pink, 4:00, orange, 4, 4:50, red *Stopped at 7:16
5	N/A	N/A	N/A	N/A	N/A	N/A
6	N/A	N/A	N/A	N/A	N/A	N/A
7	N/A	N/A	N/A	N/A	N/A	N/A
8	1	Stereo	1, 1:04, blue, tree - stopped at 1:53	N/A	N/A	N/A
9	2	Stereo	1,1:08, red, right tree, 2, 1:40, red, back tree, 3, 3:02, pink,	N/A	N/A	N/A

			tree to left, 4, 4:27, orange, tree to right, 5, 5:29, blue, tree to left, stop at 6:29			
10	N/A	N/A	N/A	N/A	N/A	N/A
11	1	Mono	[1:10, Red, Bridge], [4:05, pink, small bridge], [4:36, pink, trees], [5:40, red, trees + rocks], [6:45, pink, ridge], [7:07, blue, tree/grove], [8:30, orange, lake by trees], [9:31, blue, ridge by trees]	2	Stereo	[1:00, pink, trees], [1:29, pink, other trees], [2:20 pink, ridge by lake], Stopped at 2:30
12	2	Stereo	pink at 2:02, red at 5:05, light blue at 9:47	1	Mono	red at 0:21, gray-blue at 1:35, pink at 2:50, pink at 3:13, grey at 4:25, red at 5:28, grey at 6:50, green at 9:55 comments: "definitely easier to fly in VR", "easier to scan"

13	2	Stereo	Quit after 2 minutes	1	Mono	red at 1:43, pink at 2:00 - felt sick 2 minutes into VR on SAT test 2. with mono had difficulty orienting UAV to find figures, oculus easier to look around with
14	1	Mono	[0.23, Red, Highway], [1:33, Grey/Blue, Tree], [2:35, Green, Tree], [3:46, Pink, Highway], [4:04, pink, 5, Tree], [5:39, blue, 12, tree], [6:57, red, 13, tree], [8:23, orange, 14, by the lake/tree], [9:40, blue , tree], [9:59, blue, tree]	2	Stereo	N/A
15	1	Mono	1,0:37, red, bridge, 2, 1:25, blue, between 2 trees, 3, 2:08, pink, bridge	2	Stereo	1, 1:50, no color, between 2 trees, 2, 3:25, pink, tree, 3, 4:17, no

						color foun, tree, 4, 4:49, no color, tree, 5, 5:14, blue, tree
16	N/A	N/A	N/A	N/A	N/A	N/A
17	1	Stereo	Stopped at 0:43 (felt sick)	N/A	N/A	N/A
18	1	Stereo	red at 0:19, light blue at 1:48, pink at 4:08, pink at 5:06, orange at 7:20	2	Mono	pink at 1:20, pink at 5:33, brown at 6:17, pink at 8:12 - VR immersiveness made it "easier to get the controls down"

Appendix E-5: Movement Survey Responses

	Q1: Overall, which test did you feel more comfortable with?	Q2: In your opinion, which test more accurately mimicked human vision?	Q3: Which test did you feel you did better on (e.g. completed course more quickly, ran into fewer obstacles)?	Q5: Overall, which test did you like better?
Monoscopic	6	4	4	4
Stereoscopic	7	8	9	7
Both Equally	1	2	1	3

Appendix E-6: Search and Rescue Survey Responses

	Q1: Overall, which test did you feel more comfortable with?	Q2: In your opinion, which test more accurately mimicked human vision?	Q3: Which test did you feel you did better on (e.g. completed course more quickly, ran into fewer obstacles)?	Q5: Overall, which test did you like better?
Monoscopic	5	1	5	4
Stereoscopic	1	6	2	2
Both	1	0	0	1

Appendix F: Initial Range Test Procedures

1. Set up the Connex transmitter and receiver at setup location following manufacturer instructions.
2. Set both GoPros to a resolution of 1080p, and a frame rate of 60 fps.
3. Turn on 1 connex.
4. The stationary test examiner should visually verify on the monitor that video is transmitting to monitor and that latency is acceptable. This person will remain at the monitor for the remainder of the test.
5. The mobile person picks up the UAV portion of Connex while holding the 2 antennas towards the Ground Control Station (GCS) portion.
6. Establish communication via cell phone between the stationary person and the mobile person.
7. The mobile person will record the stationary location using iPhone Coordinates app.
8. The mobile person will slowly walk towards Regents Parking Garage while communicating via cell phone (call) to stationary person until stationary person notices a change in transmission quality. The stationary person will constantly monitor the quality of the transmitted video through the monitor by visually observing for a loss of signal or a change in latency or pixelation making notes of what occurs.
9. When the stationary person notices a change, they will communicate to the mobile person to stop. The mobile person will stop moving and will then record their current location using the iPhone Coordinates app. Repeat as necessary to verify the range, making note of findings.
10. Return to the stationary location and turn on the 2nd Connex. Repeat steps 4-9.

The materials and setup of the equipment are shown in Figures 32-34, with the UAV portion of the system in the box in Figure 34, and the stationary setup in Figure 33.

Figure 32: Initial Connex communication test materials including: a GoPro, 2 Connex transmitters and antenna located in the hand, and 2 Connex receivers and a monitor located on the table.

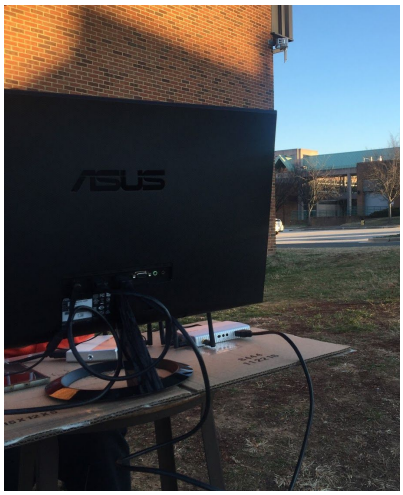

Figure 33: Initial Connex communication test stationary setup.

Figure 34: Initial Connex communication test mobile UAV portion Connex setup.

References

[1] F. Barbash, "Watch as drone helps rescue boys caught in 9-foot ocean swell," *Washington Post*, 19-Jan-2018.

[2] R. R. Murphy *et al.*, "Search and Rescue Robotics," in *Springer Handbook of Robotics*, Springer, Berlin, Heidelberg, 2008, pp. 1151–1173.

[3] J. L. Burke, R. R. Murphy, M. D. Coovert, and D. L. Riddle, "Moonlight in Miami: Field Study of Human-Robot Interaction in the Context of an Urban Search and Rescue Disaster Response Training Exercise," *Human–Computer Interaction*, vol. 19, no. 1–2, pp. 85–116, Jun. 2004.

[4] Michigan Citizen Corps Council. "COMMUNITY EMERGENCY RESPONSE TEAM Participant Handbook 2." Federal Emergency Management Agency Emergency Management Institute, March-2003.

[5] Y. Liu and G. Nejat, "Robotic Urban Search and Rescue: A Survey from the Control Perspective," *Journal of Intelligent & Robotic Systems; Dordrecht*, vol. 72, no. 2, pp. 147–165, Nov. 2013.

[6] M. Erdelj, E. Natalizio, K. R. Chowdhury, and I. F. Akyildiz, "Help from the Sky: Leveraging UAVs for Disaster Management," *IEEE Pervasive Computing*, vol. 16, no. 1, pp. 24–32, Jan. 2017.

[7] "Aeryon SkyRanger Features." *Aeryon Labs Inc.*

[8] "Draganflyer X4-ES Four Rotor UAV Helicopter Aerial Video Platform." [Online]. Available: http://www.draganfly.com/uav-helicopter/draganflyer-x4es/. [Accessed: 17-Sep-2015].

[9] “Indago UAV.” [Online]. Available: http://www.lockheedmartin.com/us/products/procerus/quad-vtol.html. [Accessed: 17-Sep-2015].

[10] “md4-1000: weather-resistant, robust and powerful drone.” [Online]. Available: http://www.microdrones.com/en/products/md4-1000/technical-data/. [Accessed: 17-Sep-2015].

[11] “Qube: Small UAS - AeroVironment, Inc.” [Online]. Available: http://www.avinc.com/uas/small_uas/qube. [Accessed: 29-Sep-2015].

[12] “SkyJib-X4 Ti-QR – Payload Weight Class 1000-2500 grams (2-5.5 Lbs) | Aeronavics – Advanced Aerial Solutions.” *Aeronavics - Advanced Aerial Solutions*. [Online]. Available: http://aeronavics.com/products/shop/rtf-packages/skyjib-x4-titanium/. [Accessed: 29-Sep-2015].

[13] American Red Cross, IBM, and Lockheed Martin. “Drones for Disaster Response and Relief Operations.” Apr-2015. [Online]. Available: http://www.zurichna.com/internet/zna/SiteCollectionDocuments/en/RIMS/drones-for-disaster-response-relief-operations-study.pdf.

[14] C. Graff. “Drone Piloting Study.” Universit`a della Svizzera Italiana, June-2014. http://juxi.net/papers/by/students/2014BSc.ChrstineGraff.pdf.

[15] G. Natarajan. “Ground control stations for unmanned air vehicles (Review Paper).” *Defence Science Journal*, vol. 51, no. 3, p. 229, May 2001.

[16] D. Labonte, P. Boissy, and F. Michaud. “Comparative Analysis of 3-D Robot Teleoperation Interfaces With Novice Users.” *IEEE Transactions on Systems, Man, and Cybernetics, Part B: Cybernetics* 40, no. 5 (October 2010): 1331–42. doi:10.1109/TSMCB.2009.2038357.

[17] M. Antunes and G. Biala, “The novel object recognition memory: neurobiology, test procedure, and its modifications,” *Cogn Process*, vol. 13, no. 2, pp. 93–110, Dec. 2011.

[18] H. Martins, I. Oakley, and R. Ventura, “Design and evaluation of a head-mounted display for immersive 3D teleoperation of field robots,” *Robotica*, vol. FirstView, pp. 1–20, May 2014.

[19] W. L. Aylsworth, H. J. Postley, B. B. Sandrew, B. E. Dobrin, and W. Husak, “Stereographic Digital Cinema: Production and Exhibition Techniques in 2012,” *Proceedings of the IEEE*, vol. 101, no. 1, pp. 169–189, Jan. 2013.

[20] R. Yao, T. Heath, A. Davies, T. Forsyth, N. Mitchell, and P. Hoberman, "Oculus VR Best Practices Guide," Oculus VR, 2015.

[21] H. Martins and R. Ventura. “Immersive 3-D teleoperation of a search and rescue robot using a head-mounted display,” in *IEEE Conference on Emerging Technologies Factory Automation, 2009. ETFA 2009*, 2009, pp. 1–8.

[22] J. M. Hillis, S. J. Watt, M. S. Landy, and M. S. Banks, “Slant from texture and disparity cues: Optimal cue combination,” *Journal of Vision*, vol. 4, no. 12, pp. 1–1, Dec. 2004.

[23] “Foundations of Cyclopean Perception,” *MIT Press*. [Online]. Available: https://mitpress.mit.edu/books/foundations-cyclopean-perception. [Accessed: 01-Dec-2015].

[24] S. Boustila, D. Bechmann, and A. Capobianco, “Effects of stereo and head tracking on distance estimation, presence, and simulator sickness using wall screen in architectural project review,” in *2017 IEEE Symposium on 3D User Interfaces (3DUI)*, 2017, pp. 231–232.

[25] J. P. McIntire, P. R. Havig, and A. R. Pinkus, “A guide for human factors research with stereoscopic 3D displays,” 2015, vol. 9470, p. 94700A–94700A–12.

[26] J. Fox, D. Arena, and J. N. Bailenson. “Virtual reality: A survival guide for the social scientist.” *Journal of Media Psychology: Theories, Methods, and Applications*, vol. 21, no. 3, pp. 95–113, 2009.

[27] B. F. Goldiez, A. M. Ahmad, and P. A. Hancock. “Effects of Augmented Reality Display Settings on Human Wayfinding Performance.” *IEEE Trans. Syst. Man Cybern. Part C Appl. Rev.*, vol. 37, no. 5, pp. 839–845, Sep. 2007.

[28] P. R. Desai, P. N. Desai, K. D. Ajmera, and K. Mehta. “A Review Paper on Oculus Rift-A Virtual Reality Headset.” *ArXiv14081173 Cs*, Aug. 2014.

[29] R.Yao, T. Heath, A. Davies, T. Forsyth, N. Mitchell, and P. Hoberman. “Oculus VR Best Practices Guide.” Oculus VR, Sep. 2014.

[30] “Oculus Rift Specs - DK1 vs DK2 comparison,” *Rift Info*.

[31] “VR Sickness, The Rift, and How Game Developers Can Help.” [Online]. Available: https://developer.oculus.com/blog/vr-sickness-the-rift-and-how-game-developers-can-help/. [Accessed: 15-Sep-2015].

[32] “Recommended System Specifications | Oculus Support Center.” [Online]. Available: https://support.oculus.com/1773584749575567/. [Accessed: 30-Mar-2018].

[33] S. Hughes, J. Manojlovich, M. Lewis, and J. Gennari. “Camera control and decoupled motion for teleoperation,” in *IEEE International Conference on Systems, Man and Cybernetics, 2003*, 2003, vol. 2, pp. 1339–1344 vol.2.

[34] H. Martins and R. Ventura. “Immersive 3-D teleoperation of a search and rescue robot using a head-mounted display,” in *IEEE Conference on Emerging Technologies Factory Automation, 2009. ETFA 2009*, 2009, pp. 1–8.

[35] K. Kruckel, F. Nolden, A. Ferrein, and I. Scholl. “Intuitive visual teleoperation for UGVs using free-look augmented reality displays,” in *2015 IEEE International Conference on Robotics and Automation (ICRA)*, 2015, pp. 4412–4417.

[36] C. W. Nielsen, M. A. Goodrich, and R. J. Rupper. “Towards facilitating the use of a pan-tilt camera on a mobile robot,” in *IEEE International Workshop on Robot and Human Interactive Communication, 2005. ROMAN 2005*, 2005, pp. 568–573.

[37] C. Furmanski, R. Azuma, and M. Daily, “Augmented-reality visualizations guided by cognition: perceptual heuristics for combining visible and obscured information,” in *International Symposium on Mixed and Augmented Reality, 2002. ISMAR 2002. Proceedings*, 2002, pp. 215–320.

[38] M. Draper, G. Calhoun, J. Nelson, and H. Ruff, "Evaluation of Synthetic Vision Overlay Concepts for UAV Sensor Operations: Landmark Cues and Picture-in-Picture," Feb. 2006.

[39] R. Azuma and C. Furmanski, "Evaluating Label Placement for Augmented Reality View Management," in *Proceedings of the 2Nd IEEE/ACM International Symposium on Mixed and Augmented Reality*, Washington, DC, USA, 2003, p. 66–.

[40] T. Höllerer, S. Feiner, D. Hallaway, B. Bell, M. Lanzagorta, D. Brown, S. Julier, Y. Baillot, and L. Rosenblum, "User interface management techniques for collaborative mobile augmented reality," *Computers & Graphics*, vol. 25, no. 5, pp. 799–810, Oct. 2001.

[41] E. Rosten, G. Reitmayr, and T. Drummond, "Real-Time Video Annotations for Augmented Reality," in *Advances in Visual Computing*, G. Bebis, R. Boyle, D. Koracin, and B. Parvin, Eds. Springer Berlin Heidelberg, 2005, pp. 294–302.

[42] E. Gans, D. Roberts, M. Bennett, H. Towles, A. Menozzi, J. Cook, and T. Sherrill. "Augmented reality technology for day/night situational awareness for the dismounted Soldier." 2015, vol. 9470, pp. 947004–947004–11.

[43] R. P. Darken and B. Peterson. "Spatial orientation, wayfinding, and representation," in *Handbook of Virtual Environments: Design, Implementation, and Applications*, K. Stanney, Ed. Mahwah, NJ: Erlbaum Associates, pp. 493–518.

[44] T. Gunther, I. S. Franke, and R. Groh, “Aughanded Virtuality - the hands in the virtual environment,” in *2015 IEEE Symposium on 3D User Interfaces (3DUI)*, 2015, pp. 157–158.

[45] A. Syberfeldt, O. Danielsson, M. Holm, and L. Wang, “Visual Assembling Guidance Using Augmented Reality,” *Procedia Manufacturing*, vol. 1, pp. 98–109, 2015.

[46] T. Waltemate, F. Hülsmann, T. Pfeiffer, S. Kopp, and M. Botsch, “Realizing a Low-latency Virtual Reality Environment for Motor Learning,” in Proceedings of the 21st ACM Symposium on Virtual Reality Software and Technology, New York, NY, USA, 2015, pp. 139–147.

[47] D. Le Gall, “MPEG: A Video Compression Standard for Multimedia Applications,” Communications of the ACM, vol. 34, no. 4, pp. 46–58, Apr. 1991.

[48] (2013). White Paper: Understanding-and Reducing- Latency in Video Compression Systems [Online]. Available: http://www.cast-inc.com/blog/white-paper-understanding-and-reducing-latency-in-video-compression-systems

[49] J. Chen, E. Haas and M. Barnes, 'Human Performance Issues and User Interface Design for Teleoperated Robots', IEEE Trans. Syst., Man, Cybern. C, vol. 37, no. 6, pp. 1231-1245, 2007.

[50] “What we do.” [Online]. Available: https://www.faa.gov/about/mission/activities/. [Accessed: 01-Dec-2015].

[51] “Certificates of Waiver or Authorization (COA).” [Online]. Available: https://www.faa.gov/about/office_org/headquarters_offices/ato/service_units/systemops/aaim/organizations/uas/coa/. [Accessed: 01-Dec-2015].

[52] Federal Aviation Administration, “Sample COA Application.” [Online]. Available: http://www.ecfr.gov/cgi-bin/text-idx?node=14:1.0.1.3.9#se14.1.21_1191. [Accessed: 01-Dec-2015].

[53]Goven, Reginald C. (2016, May).“Educational Use of Unmanned Aircraft System (UAS)” [Memorandum]. Federal Aviation Administration. Available: https://www.faa.gov/uas/resources/uas_regulations_policy/media/interpretation-educational-use-of-uas.pdf.

[54] “Powering the Rift.” [Online]. Available: https://www.oculus.com/blog/powering-the-rift. [Accessed: 13-Oct-2015].

[55] “Standard Test Method for Determining Visual Acuity and Field of View of On-Board Video Systems for Teleoperation of Robots for Urban Search and Rescue Applications, Active Standard ASTM E2566.” 2008.

[56] “Meet the ZED Stereo Camera | Stereolabs.” [Online]. Available: https://www.stereolabs.com/zed/. [Accessed: 31-Mar-2018].

[57] S. LaValle, “Sensor Fusion: Keeping It Simple.” [Online]. Available: https://developer.oculus.com/blog/sensor-fusion-keeping-it-simple/. [Accessed: 30-Mar-2018].

[58] “CONNEX User Guide,” Mar-2015. [Online]. Available: https://www.mikrocontroller.com/images/Amimon%20CONNEX%20User%20Guide_EN.pdf. [Accessed: 06-Mar-2018].